Opinion: The Germicidal Effect of Ambient Air (Open Air Factor) Revisited

R. Anthony Cox[1], Markus Ammann[2*], John N. Crowley[3*], Paul T. Griffiths[4], Hartmut Herrmann[5], Erik H. Hoffmann[5], Michael E. Jenkin[6*], V. Faye McNeill[7], Abdelwahid Mellouki[8], Christopher J. Penkett[9], Andreas Tilgner[5], and Timothy J. Wallington[10]

[1]Centre for Atmospheric Science, Department of Chemistry, University of Cambridge, Cambridge CB2 1EP, UK
[2]Laboratory of Environmental Chemistry, Paul Scherrer Institut, 5232 Villigen, Switzerland
[3]Division of Atmospheric Chemistry, Max Planck Institute for Chemistry, 55128 Mainz, Germany
[4]National Centre for Atmospheric Science, Department of Chemistry, Cambridge University, Cambridge, CB21EW, UK.
[5]Atmospheric Chemistry Department (ACD), Leibniz Institute for Tropospheric Research (TROPOS), 04318 Leipzig, Germany
[6]Atmospheric Chemistry Services, Okehampton, Devon, EX20 4QB, UK
[7]Department of Chemical Engineering, Columbia University, New York, NY 10027, USA
[8]ICARE-CNRS, 45071 Orléans CEDEX 2, France
[9]NIHR BioResource for Translational Research, University of Cambridge, Hills Road, Cambridge CB2 0QQ, UK
[10]Ford Motor Company, Research and Advanced Engineering, Dearborn, MI 48121-2053, USA

Correspondence to: Markus Ammann (markus.ammann@psi.ch), John N. Crowley (john.crowley@mpic.de), Michael E. Jenkin (atmos.chem@btinternet.com)

Abstract. The term Open-Air Factor (OAF) was coined following microbiological research in the 1960s and 1970s which established that rural air had powerful germicidal properties and attributed this to Criegee intermediates formed in the reaction of ozone with alkenes. We have re-evaluated those early experiments applying the current state of knowledge of ozone-alkene reactions. Contrary to previous speculation, neither Criegee intermediates, nor the HO radicals formed in their decomposition, are directly responsible for the germicidal activity attributed to the OAF. We identify other potential candidates, which are formed in ozone-alkene reactions and have known (and likely) germicidal properties, but the compounds responsible for the OAF remain a mystery. There has been very little research into the OAF since the 1970s and this effect seems to have been largely forgotten. In this opinion piece we remind the community of the germicidal open-air factor. Given the current global pandemic spread by an airborne pathogen, understanding the natural germicidal effects of ambient air, solving the mystery of the open-air factor, and determining how this effect can be used to improve human welfare should be a high priority for the atmospheric science community.

TOC Graphic
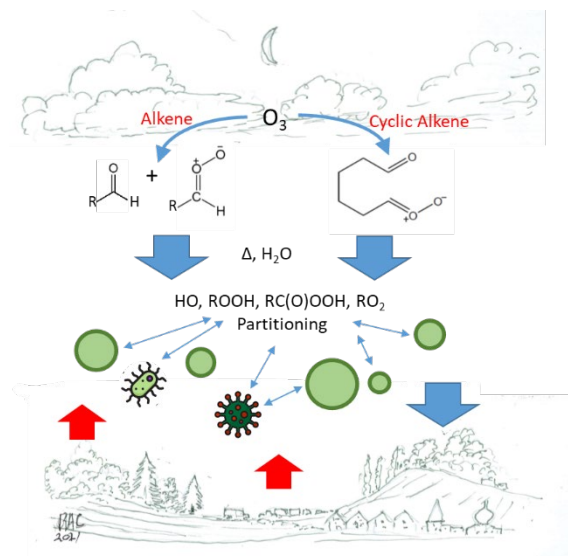
1 The history of the Open Air Factor

The public health benefits of fresh air have been recognized since ancient times (Brimblecombe, 1995; Hobday, 2019). In the 20th century, knowledge has especially evolved during major medical emergencies, such as in wartime (Souttar, 1915; Nelson, 1915; Hobday, 1997), during the 1918 influenza pandemic (Hobday and Cason, 2009) or in the treatment of tuberculosis (Ransome, 1958; Ransome and Delphine, 1894). Fresh air was also considered for theas a potential mass treatment of for burns potentially occurring during a nuclear war (Blocker et al., 1951; Artz et al., 1953). Germicidal effects of fresh air wasere also addressedinvestigated in developments ofas part of biodefence research in the 1970s biological weaponry (Hood, 2009). Furthermore, fFresh air has been considered an option in dealing with antimicrobial resistance (Wang et al., 2020). and polluted air has been found to contain Pphytotoxicins and to have germicidal effects were related to the presence of pollutants produced during photochemical smog episodes in Los Angeles (Arnold, 1959; Druett and Packman, 1968). In experiments carried out at the Microbiological Research Establishment at Porton Down (MREPD) in southern England, Druett and May (1968) reported detection of a reactive airborne species in rural air, which possessed powerful germicidal properties and called this the Open Air Factor (OAF). Flowing ambient air over microorganisms supported on spiders-web filaments resulted in a loss of viability, which was reduced to zero after ~3 hours of exposure unless the air was first passed through a brass tube, which removed the germicidal agent (hence the term Open Air). Laboratory experiments exposing *Escherichia coli* to ozone, sulphur dioxide (SO_2), nitrogen oxides (NO_X), formaldehyde (HCHO), and ionised air at ambient levels showed that none of these were the responsible agent, and fluctuations of temperature and RH were also ruled out. Exposure to direct sunlight did however kill the microorganisms, so the experiments were carried out at night-time.

Druett and May (1968) postulated that the OAF was identical, or closely related, to the "ozone-olefin complex" identified earlier in phytotoxic air pollution. This postulate was supported by additional laboratory work at the Microbiological Research Establishment at Porton Down (MREPD) by Dark and Nash (1970) who showed that the

ozonolysis of a series of alkenes resulted in significant, but variable, inactivation of *E. coli* and *Micrococcus albus*. It was not the first time that alkene ozonolysis was related to germicidal effects, as ozonated unsaturated oils have long been known as simple disinfectants (Harada, 1934; H., 1934; Travagli et al., 2010; Ugazio et al., 2020). Dark and Nash suggested that peroxide zwitterions (now known as Criegee intermediates) formed in the reaction of ozone with alkenes were the active agent of the OAF. Later work at MREPD by Hood (1974) further examined the effect of containment and found that the minimum rate of ventilation required to preserve OAF was correlated with the surface-to-volume area of the vessels used, consistent with Druett and May's idea that the OAF was removed at surfaces. Treating the OAF as a single or a small set of molecules in the gas phase enabled estimation of the diffusion coefficient of the elusive species to be made and thus the constraint of its molecular weight to the range 50-150. De Mik and De Groot (1978) at the Medical Biological Laboratory (TNO, Rijkswike, The Netherlands) found substantial damage to the DNA in aerosolized *E. coli* after exposure to air containing ozonized cyclohexene, indicating that OAF(s) could enter the outer lipid/or fatty- acid protective layer(s) of the microorganisms and that they or free radicals deriving from them are accessing and interacting chemically with DNA within the cell. Note that DNA may additionally be protected by histone proteins (Willenbrock and Ussery, 2004). Very little additional work related to the OAF has been performed since the 1970s (Hobday, 2019). A few recent studies have attempted to generate OAF to act against aerosolized microbes in the context of food preservation (Bailey et al., 2007; Nicholas et al., 2013) without providing new insight into the identity of the active agent.

Based on recent advances in our understanding of the formation and fate of Criegee intermediates in alkene-O_3 reactions (Cox et al., 2020) we show here that, contrary to previous speculation, neither Criegee intermediates, nor the HO radicals formed in their decomposition, are directly responsible for the germicidal activity attributed to the OAF but identify other potential candidates, which are formed from O_3-alkene reactions and which have known germicidal properties. The overall sequence of processes involved in the germicidal action of OAF is expected to be initiated by the reaction of ozone with alkenes producing oxygenated products in the gas phase that undergo transfer to the lipid membrane of the microorganism, where they may produce free radicals that initiate and propagate lipid phase oxidation processes. While the formation of the key species from alkene-O_3 reactions has been demonstrated experimentally, it is likely that the same species (and/or similar species) are also formed from additional pathways in ambient air (e.g. HO or NO_3 initiated oxidation of volatile organic compounds) with a number of sources therefore contributing to OAF.

2 Revisiting the Open Air Factor

The experiments of Dark and Nash (1970) provide a basis for examining germicidal agent formation in relation to what is currently known about the mechanism of alkene ozonolysis. Dark and Nash investigated the effect of a series of reactive ozone/alkene mixtures on both *E. coli* and *Micrococcus albus* suspended on micro-threads produced by spiders, to mimic airborne particles, in a 670 litre aluminium box. They selected a series of terminal alkenes, internal alkenes and cycloalkenes (and some unsaturated oxygenates). Experiments were carried out with 4 ppb, 11 ppb, and 33 ppb ozone, with alkene concentrations chosen such that 75 % ozone decay occurred over a period of 10 minutes. As shown in the supporting information (section 1), the rate coefficients for reactions of ozone with alkenes inferred

from the data reported by Dark and Nash are generally consistent with current recommended kinetic data (Cox et al., 2020) so that the relationship between germicidal effects and structure of the alkene precursor reflected the differences in oxidation pathways and in OAF yields. A key result from Dark and Nash was the observation that (through their ozonolysis) cycloalkenes appeared to be more lethal to the microorganisms than linear acyclic alkenes, which, in turn, had a greater impact than branched acyclic alkenes. It is noted that the cycloalkenes are structurally similar to some common environmental terpenoid VOCs (e.g. α-pinene, limonene). The relative efficiency (expressed as an effective loss rate coefficient, k_{loss} for the *E. coli*) of selected alkene-O$_3$ mixtures is summarised in Fig. 1, illustrating the observed range of impacts. The derivation of k_{loss} from the original data is described in the SI (section 2). These may be compared with a value of $k_{loss} \approx 0.03$ min^{-1} that can be inferred for open air for the typical conditions of the Druett and May (1968) study, based on information presented in Fig. 1 of their paper. The average values of k_{loss} for the three ozone regimes in the Dark and Nash (1970) experiments, based on the data for the alkenes shown in Fig. 1, are about 0.04, 0.09 and 0.2 min^{-1} for the 4, 11 and 33 ppb ozone experiments respectively. In approximate terms, this suggests that the germicidal agent is formed, on average, at comparable levels to the ambient level in the 4 ppb experiments, and approaching an order of magnitude higher in the 33 ppb experiments – although with substantial variation between the different alkene-O$_3$ systems.
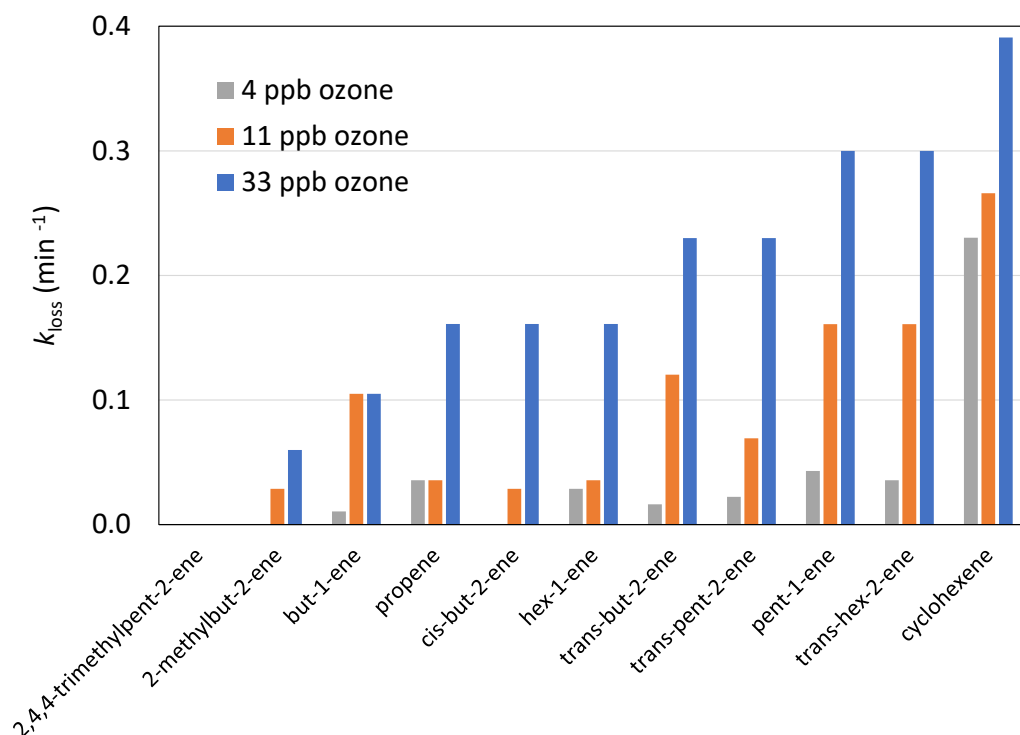

Figure 1. Average *E. coli* loss rate (k_{loss}) during the ozonolysis of selected alkenes in the experiments of Dark and Nash (1970), illustrating the variation of loss efficiency with alkene structure and ozone mixing ratio.

It is now well understood that the highly exothermic reaction of ozone with alkenes produces nascent Criegee intermediates (R1CR2OO*) with substantial internal excitation. These can either be stabilized by transferring energy

in collisions with other gas phase atmospheric species (mainly N_2 and O_2) or undergo rapid unimolecular decomposition or internal rearrangement (Donahue et al., 2011). The yield of stabilized Criegee intermediates varies greatly (Cox et al., 2020). In the case of the reactions of O_3 with cyclopentene, cyclohexene and cycloheptene, the yield is reported to be close to zero (Hatakeyama et al., 1984; Drozd and Donahue, 2011) and systematically lower than those for similarly sized acyclic alkenes. The observation by Dark and Nash that cycloalkenes are the most potent source of OAF, combined with our current understanding that there is a limited yield of stabilized Criegee intermediates formed in these systems, therefore rules out gas-phase Criegee intermediates as being the germicidal agent(s) in the OAF.

This conclusion can also be drawn from a kinetic perspective when examining the experiment by Druett and May (1968). If the germicidal agent were tied to the concentration of Criegee intermediates entering the tube from the atmosphere, it would be in steady state given by a balance between production from ozonolysis and removal via loss by unimolecular decomposition, reaction with trace gases and particles present in the air, and loss at the tube walls. As shown in the supporting materials (section 3), the lifetimes of common Criegee Intermediates with respect to gas phase sinks are < 60 ms. The same kinetic argument also holds for HO radicals, generated from decomposition of (excited or stabilized) Criegee intermediates, which are removed by gas-phase reaction with most atmospheric trace species. The typical lifetime of HO radicals in clean background UK air is about 200 ms (Lee et al., 2009; Ingham et al., 2009). Thus, the species controlling the lifetime of the bacteria in the Druett and May experiment must be related to the precursors (O_3) or the oxidation products that are lost to the walls. The kinetics of loss of viability observed in the brass tube experiments of Druett and May (Fig. S2) may provide indications for the chemical properties of the OAF, when assuming that these are volatile gas phase molecules taken up to the bacteria in a reactive process, and that the loss of these species at the wall controls the observed decay of germicidal activity. As shown in the SI (section 4), based on the experimental gas flow rates and making reasonable assumptions about the properties of the brass tube, the uptake coefficient (γ, the probability per collision that the OAF is irreversibly lost at the cylindrical wall), falls in the range of 10^{-4} to 10^{-2}. One possible explanation for the observed loss of bactericidal activity along the flow tube is loss of the precursor O_3 to the brass walls. However, γ values for O_3 are much lower than 10^{-4} (Crowley et al., 2010), especially when considering passivation effects over the several hours of the experiment. Peroxides, which are important products formed in alkene ozonolysis (and present in outside air from a variety of sources: see section 3 of the SI), are well established disinfectants (Kampf et al., 2020), and hence are potential contributors to the OAF. Oxygenated VOCs (such as peroxides) in general strongly partition (reversibly and irreversibly) to tube walls (Deming et al., 2019). As discussed in the SI (section 4), γ values for peroxides indeed fall into the range derived above to explain the wall loss rates of the Druett and May experiment. The same is true for HO_2 and possibly other peroxy radicals that could be precursors for further radicals.

To gain insight into the potential contribution of e.g. peroxy radicals and peroxides to the germicidal activity of OAF we simulated the Dark and Nash experiments. Initial scoping simulations used the detailed alkene chemistry in the "Master Chemical Mechanism" [MCM v3.2: http://mcm.york.ac.ukhttp://mcm.leeds.ac.uk/MCMv3.2/] for six of the linear acyclic alkene systems studied. The analysis not only generated gas-phase concentrations of product species, but also calculated respective vapour pressures and octanol-water partition coefficients (see SI, section 5). These

parameters are important as they impact partitioning to the condensed phase and the ability to penetrate cell membranes (see discussion below in Sect. 3). The simulations revealed that the concentrations of HO were suppressed by the high concentrations of alkenes. HO concentrations in the 33 ppb O_3 experiments were $(0.28 - 8.5) \times 10^5$ molecule cm^{-3}, with proportionately lower values in the 11 ppb and 4 ppb O_3 experiments. These were, therefore, generally lower than those typically present in air during daytime, but comparable to those reported at night in UK rural air (Emmerson and Carslaw, 2009). Simulated respective concentrations of HO_2 and RO_2, $(1.3 - 1.8) \times 10^9$ and $(6.7 - 21) \times 10^9$ molecule cm^{-3} in the 33 ppb O_3 experiments, were however significantly higher than reported at night in UK rural air (Emmerson and Carslaw, 2009). As expected, some classes of non-radical products were found to be present in much higher concentrations with aldehydes, peroxides and organic acids dominating the product distribution (See Fig. S3). Important, and sometimes major, contributions to these product classes resulted from the secondary chemistry initiated by the reactions of HO with the parent alkenes. The simulations revealed no clear trend when considering the product concentrations (or the concentration scaled by vapour pressures or octanol-water distribution coefficients) with the germicidal activity for each alkene reported by Dark and Nash. These results are summarised in detail in section 5 of the SI.

As peroxides and peroxyacids (containing the –OOH group) such as H_2O_2 and peracetic acid are known germicides (Kampf et al., 2020; Kitis, 2004; Becker et al., 2017; Goyal et al., 2014) we examined their potential contribution to OAF in more detail. For this, bespoke mechanisms were written for the extended series of 11 alkenes shown in Fig. 1, which incorporated recent improvements in the current understanding of the ozonolysis chemistry (see supporting material, section 6). The results show that (unlike the OAF) the collective formation of peroxides does not vary greatly from one alkene to the next and total levels are similar in systems with low germicidal activity (e.g., 2,4,4-trimethylpent-2-ene) and in systems with high germicidal activity (e.g., cyclohexene) (Fig. 2a). The peroxide concentrations generated from the gas phase chemistry cannot thus collectively explain the trend in bacterial destruction across the series of O_3 + alkene systems. However, the peroxides formed in the various systems include a structurally diverse set of mono-, bi- and multifunctional peroxide species (see section 6 of the supporting material), which will likely possess different propensities to penetrate the protective membrane of the microorganisms and initiate oxidation (see Sect. 3). These tend to be dominated by simple β-hydroxy peroxides (formed from secondary HO chemistry) in the acyclic systems (Fig. 2c,d). In the case of cyclohexene, however, about 30 % of the simulated peroxide burden is due to a series of highly oxygenated organic molecules (HOMs) containing hydroperoxide and/or peroxy acid groups, along with aldehyde and ketone groups (Fig. 2b). The formation of HOMs occurs via an autooxidation process (Ehn et al., 2014; Hansel et al., 2018), in which peroxy radicals generated sequentially in some alkene systems can isomerize via internal H-shift reactions resulting in rapid formation of a series of products containing increasing numbers of hydroperoxide or peroxy acid groups (Crounse et al., 2013; Crounse et al., 2011; Mutzel et al., 2015; Kirkby et al., 2016). Cyclic alkenes, such as cyclohexene, tend to have higher HOM yields than most acyclic alkenes (Bianchi et al., 2019), with HOM formation mechanisms generally not being operative for small acyclic alkenes. While this idea is consistent with the observation by Dark and Nash that the most effective (or highest concentrations of) germicidal agents were produced in the ozonolysis of endo-cyclic alkenes, we note that several small acyclic alkenes (no HOMs formation) studied still exhibited notable germicidal properties. Nonetheless, given

the plethora of (germicidal) peroxide, hydroperoxide and peracid groups in HOMs, and the fact that they partition readily to the particle phase (Riva et al., 2016; Bianchi et al., 2019), we hypothesize that HOMs may contribute to the OAF.
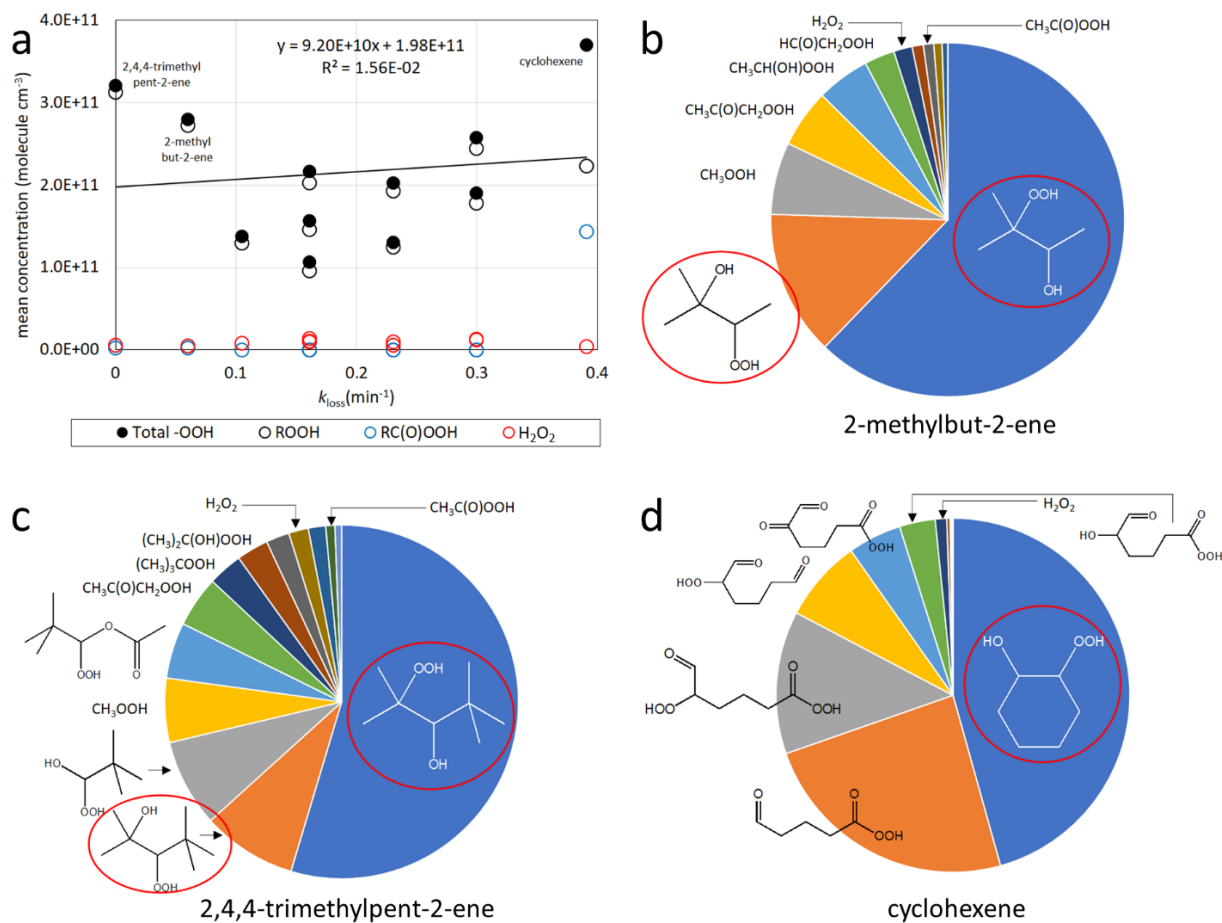

Figure 2. (a) Simulated concentrations of hydroperoxide products vs. k_{loss} for *E. coli* in 33 ppb O_3 experiments for the series of 11 alkenes shown in Fig. 1, showing the concentrations for H_2O_2, ROOH species and RC(O)OOH species and their totals (total -OOH); and linear regression of the total -OOH data. (b,c,d) Simulated speciation of peroxidic compounds generated from 2-methylbut-2-ene, 2,4,4-trimethylpent-2-ene and cyclohexene in the 33 ppb O_3 experiments. The total -OOH concentrations in the three cases were, 2.8×10^{11} 3.2×10^{11} and 3.7×10^{11} molecule cm^{-3}, respectively. Species in red ellipses are those formed from the HO + alkene reactions.

In spite of the high degree of functionalization of typical HOMs, the remaining vapor pressure could be sufficient that partitioning to the bacteria on the spider webs of the experiments and to the wall of vessels that was deduced by Hood (1974) becomes efficient. The air sampled in the Druett and May experiments certainly contained deliquesced, background aerosol on which condensation or dissolution of HOMs and other lower volatility peroxides would have occurred. At relatively high humidity, the particle – gas equilibration time-scale for an internally mixed aerosol was likely fast enough to enable the brass tube of the Druett and May experiment to act as a ~~denuder~~ sink for the HOM

and other peroxidic or oxygenated species (Deming et al., 2019), meaning that the apparent OAF wall-loss kinetics could possibly have been driven by evaporation from the particles.

3. Implications

As mentioned above, the role of hydrogen peroxide (Kampf et al., 2020; Goyal et al., 2014), organic peroxides or peracids (Becker et al., 2017; Kitis, 2004) as disinfectants for a wide range of pathogens is well established. The work of De Mik and De Groot demonstrated that DNA damage resulted from primary or secondary attack on the organisms. The organisms are protected from external damage by oxidizing agents present in the air by external membranes surrounding the internal aqueous medium containing the key chemical entities controlling the functions in the cell. The chemical nature of the membrane layer is different in individual microorganisms. *E. coli* are surrounded by a lipid membrane, as are many viruses. Other micro-organisms have chemically different protective layers. The mechanism of action of peroxides and HOMs containing peroxidic and peroxyacidic groups is likely through their oxidation potential, via their thermal decomposition to yield smaller radicals as a source of reactive oxygen species that also drives their health impact when inhaled (Tong et al., 2019). The germicidal effects of ozonated unsaturated oils has been attributed to secondary ozonides and peroxides (Travagli et al., 2010). These result from the reaction of the stabilized Criegee intermediate (produced by ozonolysis in the condensed phase) with carbonyl compounds (Bailey, 1958; Zahardis and Petrucci, 2007; Pleik et al., 2018). In a recent experimental investigation of autoxidation of unsaturated lipids initiated by gas phase HO, Zeng et al. (Zeng et al., 2020) observed substantial amplification of oxidation via lipid autoxidation propagated by Criegee intermediates and free radicals. These two examples emphasise that via pathways specific for the condensed phase, provide a routeing an example of how radical precursors, such as HOMs or peroxides in general may initiate a wealth of oxidative processes in the condensed phase. The finding of lipid membrane degradation initiated by reactive species fits with the fact that microbes with lipid membranes, including enveloped viruses and vegetative bacteria, are more susceptible to degradation by disinfectant agents than other microbes such as capsid viruses or prion proteins (Russell, 1999). The amplifying effect of radicals in lipid peroxidation also highlights that even very small amounts of OAF may have a substantial germicidal effect.

In summary, the discussion above indicates that a range of products formed in the ozonolysis of alkenes could contribute to the OAF as distinct germicides. Chemical simulations of these chemical systems do not identify a clear individual gas-phase molecule or class of molecules that matches the ranking of bactericidal activity reported in the experiments of Dark and Nash. However, we need to keep in mind that the gas phase yields of the suspected species may not correlate directly with their germicidal effects as the response of germs is related to the partitioning of these species to the condensed phase in a highly non-linear manner and may also depend on their ability to initiate condensed phase free radical chemistry that ultimately kills pathogens.

Although the airborne pathway, i.e., aerosol particles carrying pathogens and infecting a target, is recognised as a major route of transmission of many infectious diseases, including transmission of SARS-CoV-2 (Prather et al., 2020; Greenhalgh et al., 2021), the current understanding of the processes involved in the transmission of infection (e.g. during the current pandemic) is incomplete. An improved understanding of the OAF will help assessing the importance of outdoor air on the transmission of COVID-19, as well as the importance of ventilation in indoor environments

(Morawska and Milton, 2020; Morawska et al., 2020). It is therefore of substantial interest to further investigate the role of ambient air in pathogen viability and the mechanisms behind the OAF.

References

Arnold, W. N.: The longevity of the phytotoxicant produced from gaseous ozone-olefin reactions, Int. J. Air Poll., 2, 167-174, 1959.

Artz, C. P., Reiss, E., Davis, J. H. J., and Amspacher, W. H.: The exposure treatment of burns, Annals Surgery, 137, 456-464, 1953.

Bailey, P. S.: The reactions of ozone with organic compounds, Chem. Rev., 58, 925–1010, 1958.

Bailey, R., Fielding, L., Young, A., and Griffith, C.: Effect of Ozone and Open Air Factor against Aerosolized Micrococcus luteus, J. Food Prot., 70, 2769-2773, 10.4315/0362-028X-70.12.2769, 2007.

Becker, B., Brill, F. H. H., Todt, D., Steinmann, E., Lenz, J., Paulmann, D., Bischoff, B., and Steinmann, J.: Virucidal efficacy of peracetic acid for instrument disinfection, Antimicr. Res. Inf. Contr., 6, 114, 10.1186/s13756-017-0271-3, 2017.

Bianchi, F., Kurtén, T., Riva, M., Mohr, C., Rissanen, M. P., Roldin, P., Berndt, T., Crounse, J. D., Wennberg, P. O., Mentel, T. F., Wildt, J., Junninen, H., Jokinen, T., Kulmala, M., Worsnop, D. R., Thornton, J. A., Donahue, N., Kjaergaard, H. G., and Ehn, M.: Highly Oxygenated Organic Molecules (HOM) from Gas-Phase Autoxidation Involving Peroxy Radicals: A Key Contributor to Atmospheric Aerosol, Chem. Rev., 119, 3472-3509, https://doi.org/10.1021/acs.chemrev.8b00395, 2019.

Blocker, T. G. J., Blocker, V., Lewis, S. R., and Snyder, C. C.: An approach to the problem of burn sepsis with the use of open-air therapy, Annals Surgery, 134, 574-580, 1951.

Brimblecombe, P.: History of air pollution, in: Composition, Chemistry and Climate of the Atmosphere, edited by: Singh, H. B., Van Nostrand, New York, 1-18, 1995.

Cox, R. A., Ammann, M., Crowley, J. N., Herrmann, H., Jenkin, M. E., McNeill, V. F., Mellouki, A., Troe, J., and Wallington, T. J.: Evaluated kinetic and photochemical data for atmospheric chemistry: Volume VII – Criegee intermediates, Atmos. Chem. Phys., 20, 13497-13519, https://doi.org/10.5194/acp-20-13497-2020, 2020.

Crounse, J. D., Paulot, F., Kjaergaard, H. G., and Wennberg, P. O.: Peroxy radical isomerization in the oxidation of isoprene, Phys. Chem. Chem. Phys., 13, 13607-13613, https://doi.org/10.1039/C1CP21330J, 2011.

Crounse, J. D., Nielsen, L. B., Jørgensen, S., Kjaergaard, H. G., and Wennberg, P. O.: Autoxidation of Organic Compounds in the Atmosphere, J. Phys. Chem. Lett., 4, 3513-3520, https://doi.org/10.1021/jz4019207, 2013.

Crowley, J. N., Ammann, M., Cox, R. A., Hynes, R. G., Jenkin, M. E., Mellouki, A., Rossi, M. J., Troe, J., and Wallington, T. J.: Evaluated kinetic and photochemical data for atmospheric chemistry: Volume V - Heterogeneous reactions on solid substrates, Atmos. Chem. Phys., 10, 9059-9223, https://doi.org/, 2010.

Dark, F. A., and Nash, T.: Comparative toxicity of various ozonized olefins to bacteria suspended in air, Journal of Hygiene, 68, 245-252, https://doi.org/10.1017/S0022172400028710, 1970.

De Mik, G., and De Groot, I.: Breaks induced in the deoxyribonucleic acid of aerosolized Escherichia coli by ozonized cyclohexene, Applied and Environmental Microbiology, 35, 6-10, 1978.

Deming, B. L., Pagonis, D., Liu, X., Day, D. A., Talukdar, R., Krechmer, J. E., de Gouw, J. A., Jimenez, J. L., and Ziemann, P. J.: Measurements of delays of gas-phase compounds in a wide variety of tubing materials due to gas–wall interactions, Atmos. Meas. Tech., 12, 3453-3461, 10.5194/amt-12-3453-2019, 2019.

Donahue, N. M., Drozd, G. T., Epstein, S. A., Presto, A. A., and Kroll, J. H.: Adventures in ozoneland: down the rabbit-hole, Phys. Chem. Chem. Phys., 13, 10848-10857, https://doi.org/10.1039/C0CP02564J, 2011.

Drozd, G. T., and Donahue, N. M.: Pressure Dependence of Stabilized Criegee Intermediate Formation from a Sequence of Alkenes, J. Phys. Chem. A, 115, 4381-4387, https://doi.org/10.1021/jp2001089, 2011.

Druett, H. A., and May, K. R.: Unstable Germicidal Pollutant in Rural Air, Nature, 220, 395-396, https://doi.org/10.1038/220395a0, 1968.

Druett, H. A., and Packman, L. P.: Sensitive Microbiological Detector for Air Pollution, Nature, 218, 699-699, 10.1038/218699a0, 1968.

Ehn, M., Thornton, J. A., Kleist, E., Sipilä, M., Junninen, H., Pullinen, I., Springer, M., Rubach, F., Tillmann, R., Lee, B., Lopez-Hilfiker, F., Andres, S., Acir, I.-H., Rissanen, M., Jokinen, T., Schobesberger, S., Kangasluoma, J., Kontkanen, J., Nieminen, T., Kurtén, T., Nielsen, L. B., Jørgensen, S., Kjaergaard, H. G., Canagaratna, M., Maso, M. D., Berndt, T., Petäjä, T., Wahner, A., Kerminen, V.-M., Kulmala, M., Worsnop, D. R., Wildt, J., and Mentel, T. F.: A large source of low-volatility secondary organic aerosol, Nature, 506, 476, https://doi.org/10.1038/nature13032, 2014.

Emmerson, K. M., and Carslaw, N.: Night-time radical chemistry during the TORCH campaign, Atmos. Environ., 43, 3220-3226, https://doi.org/10.1016/j.atmosenv.2009.03.042, 2009.

Goyal, S. M., Chander, Y., Yezli, S., and Otter, J. A.: Evaluating the virucidal efficacy of hydrogen peroxide vapour, J. Hosp. Infect., 86, 255-259, https://doi.org/10.1016/j.jhin.2014.02.003, 2014.

Greenhalgh, T., Jimenez, J. L., Prather, K. A., Tufekci, Z., Fisman, D., and Schooley, R.: Ten scientific reasons in support of airborne transmission of SARS-CoV-2, The Lancet, https://doi.org/10.1016/S0140-6736(21)00869-2, 2021.

Hansel, A., Scholz, W., Mentler, B., Fischer, L., and Berndt, T.: Detection of RO2 radicals and other products from cyclohexene ozonolysis with NH_4^+ and acetate chemical ionization mass spectrometry, Atmos. Environ., 186, 248-255, https://doi.org/10.1016/j.atmosenv.2018.04.023, 2018.

Harada, T.: Olive Oil Ozonide and its Fungicidal Quality, Bull. Chem. Soc. Japan, 9, 192-197, https://doi.org/10.1246/bcsj.9.192, 1934.

Hatakeyama, S., Kobayashi, H., and Akimoto, H.: Gas-phase oxidation of sulfur dioxide in the ozone-olefin reactions, J. Phys. Chem., 88, 4736-4739, https://doi.org/10.1021/j150664a058, 1984.

Hobday, R. A., and Cason, J. W.: The Open-Air treatment of pandemic influenza, Am. J. Publ. Health, 99, S236-S242, 10.2105/ajph.2008.134627, 2009.

Hobday, R. A.: Sunlight therapy and solar architecture, Medical History, 41, 455-472, 10.1017/S0025727300063043, 1997.

Hobday, R. A.: The open-air factor and infection control, J. Hosp. Infect., 103, e23-e24, https://doi.org/10.1016/j.jhin.2019.04.003, 2019.

Hood, A. M.: Open-Air Factors in Enclosed Systems, J. Hyg., 72, 53-60, https://doi.org/10.1017/s0022172400023202, 1974.

Hood, A. M.: The effect of open-air factors on the virulence and viability of airborne Francisella tularensis, Epidemiol. Infect., 137, 753-761, 10.1017/S0950268809002076, 2009.

Ingham, T., Goddard, A., Whalley, L. K., Furneaux, K. L., Edwards, P. M., Seal, C. P., Self, D. E., Johnson, G. P., Read, K. A., Lee, J. D., and Heard, D. E.: A flow-tube based laser-induced fluorescence instrument to measure OH reactivity in the troposphere, Atmos. Meas. Tech., 2, 465-477, https://doi.org/10.5194/amt-2-465-2009, 2009.

Kampf, G., Todt, D., Pfaender, S., and Steinmann, E.: Persistence of coronaviruses on inanimate surfaces and their inactivation with biocidal agents, J. Hosp. Infect., 104, 246-251, https://doi.org/10.1016/j.jhin.2020.01.022, 2020.

Kirkby, J., Duplissy, J., Sengupta, K., Frege, C., Gordon, H., Williamson, C., Heinritzi, M., Simon, M., Yan, C., Almeida, J., Tröstl, J., Nieminen, T., Ortega, I. K., Wagner, R., Adamov, A., Amorim, A., Bernhammer, A.-K., Bianchi, F., Breitenlechner, M., Brilke, S., Chen, X., Craven, J., Dias, A., Ehrhart, S., Flagan, R. C., Franchin, A., Fuchs, C., Guida, R., Hakala, J., Hoyle, C. R., Jokinen, T., Junninen, H., Kangasluoma, J., Kim, J., Krapf, M., Kürten, A., Laaksonen, A., Lehtipalo, K., Makhmutov, V., Mathot, S., Molteni, U., Onnela, A., Peräkylä, O., Piel, F., Petäjä, T., Praplan, A. P., Pringle, K., Rap, A., Richards, N. A. D., Riipinen, I., Rissanen, M. P., Rondo, L., Sarnela, N., Schobesberger, S., Scott, C. E., Seinfeld, J. H., Sipilä, M., Steiner, G., Stozhkov, Y., Stratmann, F., Tomé, A., Virtanen, A., Vogel, A. L., Wagner, A. C., Wagner, P. E., Weingartner, E., Wimmer, D., Winkler, P. M., Ye, P., Zhang, X., Hansel, A., Dommen, J., Donahue, N. M., Worsnop, D. R., Baltensperger, U., Kulmala, M., Carslaw, K. S., and Curtius, J.: Ion-induced nucleation of pure biogenic particles, Nature, 533, 521, https://doi.org/10.1038/nature17953, 2016.

Kitis, M.: Disinfection of wastewater with peracetic acid: a review, Environ. Int., 30, 47-55, https://doi.org/10.1016/S0160-4120(03)00147-8, 2004.

Lee, J. D., Young, J. C., Read, K. A., Hamilton, J. F., Hopkins, J. R., Lewis, A. C., Bandy, B. J., Davey, J., Edwards, P., Ingham, T., Self, D. E., Smith, S. C., Pilling, M. J., and Heard, D. E.: Measurement and calculation of OH reactivity at a United Kingdom coastal site, J. Atmos. Chem., 64, 53-76, https://doi.org/10.1007/s10874-010-9171-0, 2009.

Morawska, L., and Milton, D. K.: It Is Time to Address Airborne Transmission of Coronavirus Disease 2019 (COVID-19), Clin. Infect. Dis., 71, 2311-2313, https://doi.org/10.1093/cid/ciaa939, 2020.

Morawska, L., Tang, J. W., Bahnfleth, W., Bluyssen, P. M., Boerstra, A., Buonanno, G., Cao, J., Dancer, S., Floto, A., Franchimon, F., Haworth, C., Hogeling, J., Isaxon, C., Jimenez, J. L., Kurnitski, J., Li, Y., Loomans, M., Marks, G., Marr, L. C., Mazzarella, L., Melikov, A. K., Miller, S., Milton, D. K., Nazaroff, W., Nielsen, P. V., Noakes, C., Peccia, J., Querol, X., Sekhar, C., Seppänen, O., Tanabe, S.-i., Tellier, R., Tham, K. W., Wargocki, P., Wierzbicka, A., and Yao, M.: How can airborne transmission of COVID-19 indoors be minimised?, Environ. Int., 142, 105832, https://doi.org/10.1016/j.envint.2020.105832, 2020.

Mutzel, A., Poulain, L., Berndt, T., Iinuma, Y., Rodigast, M., Böge, O., Richters, S., Spindler, G., Sipilä, M., Jokinen, T., Kulmala, M., and Herrmann, H.: Highly Oxidized Multifunctional Organic Compounds Observed in Tropospheric Particles: A Field and Laboratory Study, Environ. Sci. Technol., 49, 7754-7761, https://doi.org/10.1021/acs.est.5b00885, 2015.

Nelson, W. E.: Open-Air treatment for wounds, a simple and inexpensive form of Open-Air ward, as used at the V.A.D. Hospital, Henley-in-Arden, British Med. J., 2, 324-324, 10.1136/bmj.2.2852.324, 1915.

Nicholas, R., Dunton, P., Tatham, A., and Fielding, L.: The effect of ozone and open air factor on surface-attached and biofilm environmental Listeria monocytogenes, J. Appl. Microbiol., 115, 555-564, https://doi.org/10.1111/jam.12239, 2013.

Pleik, S., Spengler, B., Ram Bhandari, D., Luhn, S., Schäfer, T., Urbach, D., and Kirsch, D.: Ambient-air ozonolysis of triglycerides in aged fingerprint residues, Analyst, 143, 1197-1209, 10.1039/C7AN01506B, 2018.

Prather, K. A., Marr, L. C., Schooley, R. T., McDiarmid, M. A., Wilson, M. E., and Milton, D. K.: Airborne transmission of SARS-CoV-2, Science, 370, 303-304, https://doi.org/10.1126/science.abf0521, 2020.

Ransome, A.: Remarks on Sanatoria for the Open-Air Treatment of Consumption, British Med. J., 2, 69-73, 10.1136/bmj.2.1958.69, 1898.

Ransome A. and Delphine, S., On the influence of certain natural agents on the virulence of the tubercle-bacillus, Proc. R. Soc. Lond., 56, 51-56, 1894.

Riva, M., Budisulistiorini, S. H., Chen, Y., Zhang, Z., D'Ambro, E. L., Zhang, X., Gold, A., Turpin, B. J., Thornton, J. A., Canagaratna, M. R., and Surratt, J. D.: Chemical Characterization of Secondary Organic Aerosol from Oxidation of Isoprene Hydroxyhydroperoxides, Environ. Sci. Technol., 50, 9889-9899, https://doi.org/10.1021/acs.est.6b02511, 2016.

Russell, A. D.: Bacterial resistance to disinfectants: present knowledge and future problems, J. Hosp. Infect., 43, S57-S68, https://doi.org/10.1016/S0195-6701(99)90066-X, 1999.

Souttar HS. A Surgeon in Belgium. London: E. Arnold. 1915.

Tong, H., Zhang, Y., Filippi, A., Wang, T., Li, C., Liu, F., Leppla, D., Kourtchev, I., Wang, K., Keskinen, H.-M., Levula, J. T., Arangio, A. M., Shen, F., Ditas, F., Martin, S. T., Artaxo, P., Godoi, R. H. M., Yamamoto, C. I., de Souza, R. A. F., Huang, R.-J., Berkemeier, T., Wang, Y., Su, H., Cheng, Y., Pope, F. D., Fu, P., Yao, M., Pöhlker, C., Petäjä, T., Kulmala, M., Andreae, M. O., Shiraiwa, M., Pöschl, U., Hoffmann, T., and Kalberer, M.: Radical Formation by Fine Particulate Matter Associated with Highly Oxygenated Molecules, Environ. Sci. Technol., 53, 12506-12518, https://doi.org/10.1021/acs.est.9b05149, 2019.

Travagli, V., Zanardi, I., Valacchi, G., and Bocci, V.: Ozone and Ozonated Oils in Skin Diseases: A Review, Mediat. Inflamm., 2010, 610418, https://doi.org/10.1155/2010/610418, 2010.

Ugazio, E., Tullio, V., Binello, A., Tagliapietra, S., and Dosio, F.: Ozonated Oils as Antimicrobial Systems in Topical Applications. Their Characterization, Current Applications, and Advances in Improved Delivery Techniques, Molecules, 25, 334, 2020.

Wang, C.-H., Hsieh, Y.-H., Powers, Z. M., and Kao, C.-Y.: Defeating antibiotic-resistant bacteria: exploring alternative therapies for a post-antibiotic era, Int. J. Mol. Sci., 21, 1061, 2020.

Willenbrock, H., and Ussery, D. W.: Chromatin architecture and gene expression in Escherichia coli, Genome Biol., 5, 252-252, https://doi.org/10.1186/gb-2004-5-12-252, 2004.

Zahardis, J., and Petrucci, G. A.: The oleic acid-ozone heterogeneous reaction system: products, kinetics, secondary chemistry, and atmospheric implications of a model system - a review, Atmos. Chem. Phys., 7, 1237-1274, 2007.

Zeng, M., Heine, N., and Wilson, K. R.: Evidence that Criegee intermediates drive autoxidation in unsaturated lipids, Proc. Natl. Acad. Sci. U. S. A., 117, 4486-4490, https://doi.org/10.1073/pnas.1920765117, 2020.

Supporting information for

Opinion: The Germicidal Effect of Ambient Air (Open Air Factor) Revisited

R. Anthony Cox[1], Markus Ammann[2], John N. Crowley[3], Paul T. Griffiths[4], Hartmut Herrmann[5], Erik H. Hoffmann[5], Michael E. Jenkin[6], V. Faye McNeill[7], Abdelwahid Mellouki[8], Chris J. Penkett[9], Andreas Tilgner[5], and Timothy J. Wallington[10]

[1]Centre for Atmospheric Science, Department of Chemistry, University of Cambridge, Cambridge CB2 1EP, UK
[2]Laboratory of Environmental Chemistry, Paul Scherrer Institut, 5232 Villigen, Switzerland
[3]Division of Atmospheric Chemistry, Max Planck Institute for Chemistry, 55128 Mainz, Germany
[4]National Centre for Atmospheric Science, Department of Chemistry, Cambridge University, Cambridge, CB21EW, UK.
[5]Atmospheric Chemistry Department (ACD), Leibniz Institute for Tropospheric Research (TROPOS), 04318 Leipzig, Germany
[6]Atmospheric Chemistry Services, Okehampton, Devon, EX20 4QB, UK
[7]Department of Chemical Engineering, Columbia University, New York, NY 10027, USA
[8]ICARE-CNRS, 45071 Orléans CEDEX 2, France
[9]NIHR BioResource for Translational Research, University of Cambridge, Hills Road, Cambridge CB2 0QQ, UK
[10]Ford Motor Company, Research and Advanced Engineering, Dearborn, MI 48121-2053, USA

Correspondence to: Markus Ammann (markus.ammann@psi.ch), John N. Crowley (john.crowley@mpic.de), Michael E. Jenkin (atmos.chem@btinternet.com).

1. Kinetics of ozone + alkene reactions inferred from data presented by Dark and Nash

Rate coefficients for the gas-phase reaction of ozone with alkenes used in the experiments by Dark and Nash (1970) can be estimated from the quantity of alkene needed to produce the ozone half-life of 5 minutes. The alkenes were in excess and dividing the pseudo first order loss rate of ozone (2.31×10^{-3} s^{-1}) by the alkene concentration used in the experiments gives the bimolecular rate coefficients shown on the y-axis in Fig. S1 below. Plotted on the x-axis are the rate coefficients taken from the 2020 recommendations by IUPAC (Cox et al., 2020) and McGillen et al. (2020). As seen from Fig. S1 the rate coefficients inferred from the experimental conditions reported by Dark and Nash in 1970 are consistent with our current understanding of the kinetics of ozone + alkene reactions, within about a factor of two. This consistency lends credibility to the experiments of Dark and Nash (1970) .
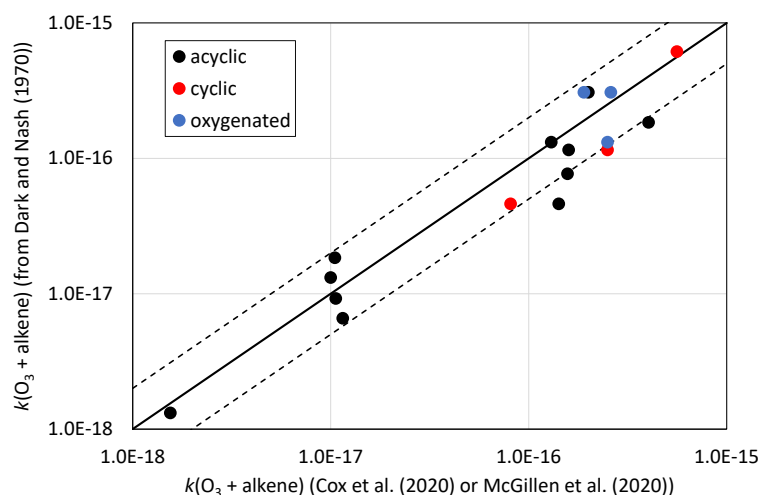
Figure S1. Rate coefficients for ozone + alkene reactions inferred from data presented by Dark and Nash (1970) plotted versus current recommendations for these reactions. The solid line represents 1:1 correspondence, the dotted lines show variation by a factor of two. The acyclic alkenes are ethene, propene, but-1-ene, pent-1-ene, hex-1-ene, *cis*-but-2-ene, *trans*-but-2-ene, *trans*-pent-2-ene*, *trans*-hex-2-ene*, 2-methylbut-2-ene, 2,4,4-trimethylpent-2-ene. The cyclic alkenes are cyclopentene, cyclohexene, and cycloheptene. The oxygenates are but-2-en-1-ol, 1-vinyloxyethane and 1-vinyloxybutane. (*Isomeric mixture used, which is dominated by *trans*- isomer).

2. Reanalysis of the data of Dark and Nash

The table below reproduces the experimental data of Dark and Nash (1970) for the selected alkenes presented in Fig. 1 of the main paper. The effects on the *Escherichia coli* population were reported as a survival fraction (*f*) following a 10 minute experimental exposure time, and a first-order loss rate constant, k_{loss} (in units of min^{-1}) is inferred here, representing the average removal rate over the 10 minute period.

Table S1. Survival fractions (*f*) of *Escherichia coli* reported by Dark and Nash (1970) for selected ozone-alkene experiments and the inferred loss rates (k_{loss}) of *Escherichia coli*.

	Survival fraction (*f*) [a]			k_{loss}/min^{-1} [b]		
[O$_3$]$_0$/ppb	33 ppb	11 ppb	4 ppb	33 ppb	11 ppb	4 ppb
cyclohexene	0.02	0.07	0.35	0.391	0.266	0.105
hex-2-ene [c]	0.05	0.20	0.70	0.300	0.161	0.036
pent-1-ene	0.05	0.20	0.65	0.300	0.161	0.043
pent-2-ene [c]	0.10	0.50	0.80	0.230	0.069	0.022
trans-but-2-ene	0.10	0.30	0.85	0.230	0.120	0.016
propene	0.20	0.70	0.70	0.161	0.036	0.036
hex-1-ene	0.20	0.70	0.75	0.161	0.036	0.029
cis-but-2-ene	0.20	0.75	1.00	0.161	0.029	0.000
but-1-ene	0.35	0.35	0.90	0.105	0.105	0.011
2-methylbut-2-ene	0.55	0.75	1.00	0.060	0.029	0.000
2,4,4-trimethylpent-2-ene	1.00	1.00	1.00	0.000	0.000	0.000

Notes:

[a] Survival fraction of *Escherichia coli* at the end of each 10 minute experiment, as reported by Dark and Nash (1970);

[b] The inferred average first-order loss rate, k_{loss}, determined from $k_{loss} = \ln(1/f)/10$ and thus assumes that mixing of gases was rapid compared to the 10 minute timescale over which the *E-coli* were exposed.

[c] Isomeric mixture dominated by *trans* isomer.

3. Characteristics of outside air at Porton Down

(a) Concentrations of NOx and volatile organic compounds (VOCs)

The experiments reported by Druett and May (1968) sampled night-time outside air at Porton Down, a rural location in southern England about 8 km north-east of Salisbury, Wiltshire (51.131, -1.704). The air composition would likely have been influenced by both local-scale chemical processes occurring shortly before sampling and regional-scale chemical processes occurring over time scales of up to a day or more prior to sampling, superimposed on northern hemispheric background air (e.g., Jenkin, 2008). Although there is no detailed information available on the air composition at that time, it is possible to estimate the approximate concentrations of some key components (NO_x and hydrocarbons) for rural southern England using more recent monitoring data from comparable rural locations (https://uk-air.defra.gov.uk/data/), and the documented trends in the emissions of air quality pollutants (https://naei.beis.gov.uk/).

The examples below (Fig. S2) show that annual mean NO_x mixing ratios have generally followed the documented trend in road transport emissions, showing a progressive decline since the early 1990s in response to EU controls of anthropogenic emissions. Based on the estimated historical trend in UK emissions shown, it can therefore be inferred that the annual mean NO_x mixing ratios at such rural locations was probably about 5 – 10 ppb at the beginning of the series in 1970. The monitoring data also show that NO accounts for about 20 % of NO_x on average at these NO_x levels, i.e., an annual mean NO mixing ratio of about 1 – 2 ppb. It should be noted that the partitioning of NO_x into NO and NO_2 shows a strong diurnal variation, with NO suppressed to very low levels at night (when regeneration by NO_2 photolysis cannot occur) by virtue of its reaction with excess O_3 (typically 20 – 25 ppb).
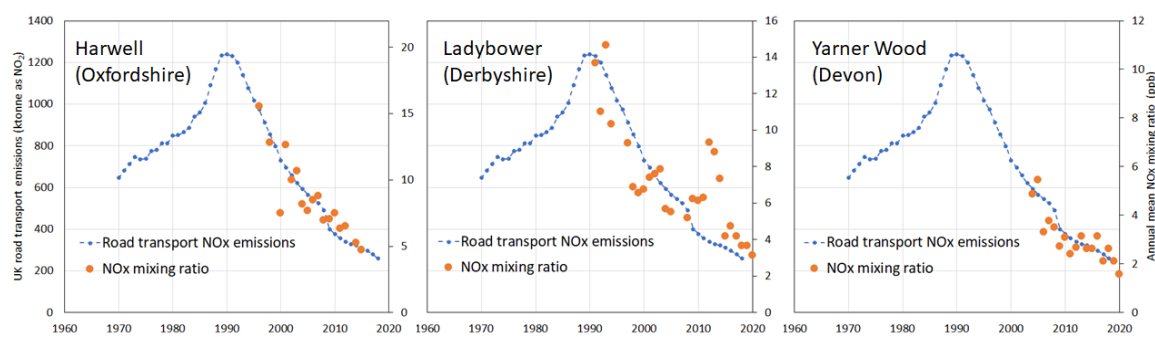
Figure S2. Comparison of the trend in UK NO_x emissions from road transport (https://naei.beis.gov.uk/) with annual mean NO_x mixing ratios measured at rural locations in the UK Automatic Urban and Rural Network, AURN (https://uk-air.defra.gov.uk/data/): Harwell, Oxfordshire (51.573, -1.316), Ladybower, Derbyshire (53.403, -1.752) and Yarner Wood, Devon (50.598, -3.717).

Concentrations of light (C_2-C_8) hydrocarbons at UK monitoring sites have also been reported to reflect the documented trend in road transport emissions, again showing a progressive decline since the early 1990s in response to EU controls

4

of anthropogenic emissions (Dollard et al., 2007). Based again on rural measurements from the Harwell site (Fig. S3), emissions trend estimates, and additionally speciation information for non-methane VOC emissions in the UK (Passant, 2002), it is possible to estimate an associated HO reactivity of about $4-5$ s^{-1} for anthropogenic non-methane VOCs in the rural southern England in 1970. The HO reactivity is expected to have been significantly further elevated by contributions from biogenic VOCs, and from oxygenated products of VOC degradation in general. It was therefore likely to have been substantially greater than the value of about 1 s^{-1}, associated with reaction with methane and CO in the remote background lower troposphere.
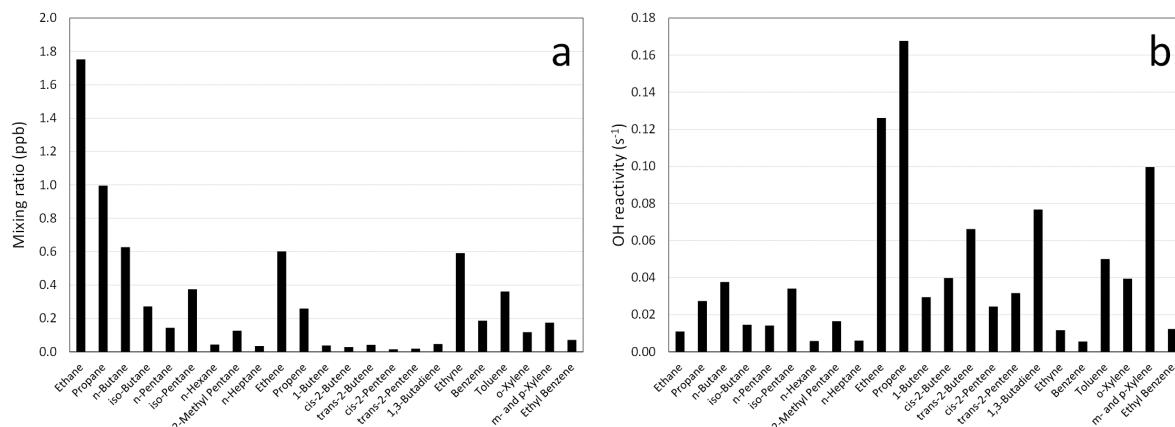
Figure S3. (a) Distribution of annual mean mixing ratios of C_2-C_8 hydrocarbons measured at Harwell, Oxfordshire (51.573, -1.316) in 2001 as part of the UK Automatic Hydrocarbon Network (https://uk-air.defra.gov.uk/data/), with the presented hydrocarbons expected to be derived predominantly from anthropogenic sources; (b) The associated HO reactivities of the measured hydrocarbons. The total HO reactivity of this VOC subset is ~1 s^{-1}, which is estimated to correspond to ~3 s^{-1} for the inferred full non-methane VOC speciation in 2001 (Passant et al., 2002); and about a factor of 1.5 greater in 1970 based on VOC emissions trends (https://naei.beis.gov.uk/).

The experiments of Druett and May (1968) were carried out after nightfall. As indicated above, the composition of the sampled air would likely have been particularly influenced by both local-scale chemical processes (e.g., O_3 and NO_3 initiated alkene oxidation), and by the air mass history over the period of a day or more, i.e., regional-scale chemical processes, including photochemically-driven HO initiated VOC chemistry. The air would therefore have been expected to contain oxygenated organic products containing a variety functional groups (including -OH, -OOH, -O-, -C(=O)-, -C(=O)O-, -ONO$_2$, -NO$_2$ and -C(=O)OONO$_2$) in addition to the radical intermediates involved in their formation mechanisms (e.g., HO, HO$_2$, RO$_2$, NO$_3$ and sCI).

(b) Formation of hydroperoxides and peroxy acids
In the present work, we have focused species containing -OOH (hydroperoxide) and -C(=O)OOH (peroxy acid) groups (in conjunction with other groups in bi- and multifunctional species), because they are known germicides. They are formed via a number of routes, including bimolecular RO$_2$ + HO$_2$ reactions, RO$_2$ isomerization (auto-oxidation) reactions, and from the reactions of stabilized Criegee intermediates (sCIs) with H$_2$O and (H$_2$O)$_2$.

The formation rate of hydroperoxides and peroxy acids from the bimolecular $RO_2 + HO_2$ reactions is determined by the ambient concentrations of the precursor RO_2 and HO_2 radicals. It is well established from modelling studies that these concentrations are relatively insensitive to the NO_x level over a wide range in the background ("methane and CO") atmosphere, with RO_2 entirely as CH_3O_2 (e.g., Logan et al., 1981; Lightfoot et al., 1992) up to about 1 ppb NO_x. At higher NO_x levels, the presence of co-emitted VOCs allows radical levels to be sustained, because reaction of HO with VOCs (forming a suite of RO_2 radicals) continues to compete with radical loss via the HO + NO_2 reaction. As indicated above, a typical HO reactivity significantly in excess of $4 - 5$ s^{-1} can be estimated for rural southern England in 1970, compared with an average reactivity of about $1 - 2$ s^{-1} for reaction with $4 - 8$ ppb NO_2 (i.e. the corresponding average estimated above). Under these conditions, conversion of HO to RO_2 and HO_2 through reaction with VOCs approximately balances the conversion of RO_2 and HO_2 to HO through reaction with NO, and the concentrations of RO_2 and HO_2 radicals thus continue to be sustained at these NO_x levels. This has been confirmed by measurements of peroxy radicals at a UK rural site by Fleming et al. (2006), which demonstrated sustained concentrations of peroxy radicals up to about $5 - 10$ ppb NO_x during day and night in both summer and winter. In addition, gaseous H_2O_2 was routinely monitored at several UK rural network sites during the late 1980s and early 1990s (i.e., the period when UK rural NO_x levels were likely at their highest), consistent with its formation (at least partially) through the operation of the $HO_2 + HO_2$ reaction (Dollard and Davies, 1992; PORG, 1993; 1997), and measurements of peroxides have been reported in many other studies at comparable NO_x levels (e.g., Zhang et al., 2012; Wang et al., 2016; Watanabe et al., 2018). Hydroperoxides and peroxy acids formed from bimolecular $RO_2 + HO_2$ reactions would therefore be expected to have been present, both in the rural air sampled by Druett and May (1968), and more generally over the intervening years. It is also noted that some relevant species (in particular peracetic acid, $CH_3C(O)OOH$: Berasategui et al., 2020) are sufficiently long-lived that their formation may have occurred on a regional-scale during the preceding day(s).

Auto-oxidation mechanisms involving RO_2 isomerization reactions (i.e., HOM formation) can also contribute to the formation of hydroperoxide and peroxy acid species, although these mechanisms can be inhibited at high NO_x by the reactions of RO_2 with NO. The pseudo-first order loss rate of peroxy radicals with respect to reaction with $1 - 2$ ppb NO (i.e., the average estimated above for rural southern England in 1970) is about $0.2 - 0.4$ s^{-1}. Because peroxy radical isomerization rates are very strongly structure dependent, this can compete with or dominate over some of the possible isomerization reactions. However, a large proportion of those calculated for peroxy radicals formed from the ozonolysis of cyclohexene (e.g., see Sect. 6) and related cyclic terpenoids are sufficiently rapid to compete with reaction with NO at this level, and all of them will certainly be competitive under the night-time conditions in the vicinity of the Druett and May (1968) sampling location, when [NO] is heavily suppressed.

The reactions H_2O and $(H_2O)_2$ with stabilized Criegee intermediates (sCIs) formed from O_3 + alkene reactions provide additional sources of both H_2O_2 and α-hydroxy hydroperoxides (e.g., Nguyen et al., 2016; Sheps et al., 2017). As discussed by Cox et al. (2020), and further below, these reactions are major loss routes for sCIs for rural conditions typical of southern England. The very rapid reactions of sCIs with organic acids (e.g., HC(O)OH: Cox et al., 2020 and references therein) and inorganic acids (HNO_3 and HCl: Foreman et al., 2016) also provide routes to products containing hydroperoxide groups (hydroperoxy-esters, nitro-oxy-hydroperoxides and chloro-hydroperoxides, respectively). Based on UK measurements of HC(O)OH (Le Breton et al., 2014; Bannan et al., 2017), HNO_3 (Le

(c) Concentrations and lifetimes of sCI

Cox et al. (2020) have recently estimated seasonally-averaged winter and summer production rates, removal rates and steady-state concentrations of sCIs, using recent observational data from the Chilbolton Observatory, (Hampshire (51.150, -1.438), southern England), which is about 15 km to the east of MRE Porton Down and in a similarly rural location. Full details are available in section 8 and Supplement C of Cox et al. (2020). The calculations made use of measured or inferred concentrations of a series of C_1–C_6 alkenes, isoprene, α-pinene, limonene, O_3, NO_2, SO_2 and HC(O)OH, in conjunction with H_2O and $(H_2O)_2$ concentrations based on modelled temperature and relative humidity data typical of the region. Production of sCIs from the ozonolysis of the C_1–C_6 alkenes, isoprene, α-pinene and limonene was therefore represented, with removal by unimolecular decomposition and bimolecular reactions with H_2O, $(H_2O)_2$, NO_2, SO_2 and HC(O)OH. These are expected to be the most important source and sink reactions (Cox et al., 2020).

Table S2. Representative ambient concentrations and lifetimes of a core set of sCIs calculated by Cox et al. (2020) for average winter conditions at the Chilbolton observatory in south-east England (T = 278 K; RH = 85 %).

sCI	Ambient concentration/ molecule cm^{-3}	Lifetime/ s	Main removal reaction
CH_2OO	5.3	5.3×10^{-4}	Reaction with $(H_2O)_2$
Z-CH_3CHOO	300	1.5×10^{-2}	Thermal decomposition
E-CH_3CHOO	2.0	9.6×10^{-5}	Reaction with $(H_2O)_2$ and H_2O
$(CH_3)_2COO$	28	5.1×10^{-3}	Thermal decomposition
Z-$(CH=CH_2)(CH_3)COO$ [a]	0.010	2.8×10^{-4}	Thermal decomposition
E-$(CH=CH_2)(CH_3)COO$ [a]	4.9	5.8×10^{-2}	Thermal decomposition
Z-$(C(CH_3)=CH_2)CHOO$ [a]	0.0042	2.7×10^{-4}	Thermal decomposition
E-$(C(CH_3)=CH_2)CHOO$ [a]	0.57	1.6×10^{-2}	Reaction with $(H_2O)_2$ and H_2O
Notes: [a] Derived specifically from isoprene.			

Tables S2 and S3 show the calculated ambient concentrations and lifetimes of a core set of sCIs for winter and summer conditions, with the total sCI concentrations being about 380 molecule cm^{-3} in both summer and winter. The core set accounted for 91 % and 76 % of the winter and summer totals, with a particularly important contribution from Z-CH_3CHOO, which is formed from all linear alk-2-enes in the alkene speciation and has a relatively long atmospheric lifetime. The main sCI removal reactions were either thermal decomposition or reaction with $(H_2O)_2$ (supplemented

by reaction with H_2O), each accounting for approximately half of total sCI loss. The calculated ambient lifetimes for all sCIs were < 60 ms in the winter and < 30 ms in the summer, with many being orders of magnitude shorter lived. The calculations of Cox et al. (2020) were based on data reported in recent years. Taking account of the trends in anthropogenic pollutant emissions discussed above (particularly for the precursor alkenes), total sCI concentrations about a factor of three higher (i.e., about 10^4 molecule cm^{-3}) can be inferred for 1970, but with their removal still dominated by the reactions shown in Tables S2 and S3 such that the lifetimes are approximately unchanged.

Table S3. Representative ambient concentrations and lifetimes of a core set of sCIs calculated by Cox et al. (2020) for average summer conditions at the Chilbolton observatory in south-east England (T = 288 K; RH = 70 %).

sCI	Ambient concentration (molecule cm^{-3})	Lifetime (s)	Main removal reaction
CH_2OO	4.5	4.2×10^{-4}	Reaction with $(H_2O)_2$
Z-CH_3CHOO	220	9.1×10^{-3}	Thermal decomposition
E-CH_3CHOO	1.5	6.0×10^{-5}	Reaction with $(H_2O)_2$ and H_2O
$(CH_3)_2COO$	19	3.4×10^{-3}	Thermal decomposition
Z-$(CH{=}CH_2)(CH_3)COO$ [a]	0.025	1.4×10^{-4}	Thermal decomposition
E-$(CH{=}CH_2)(CH_3)COO$ [a]	11	2.7×10^{-2}	Thermal decomposition
Z-$(C(CH_3){=}CH_2)CHOO$ [a]	0.010	1.3×10^{-4}	Thermal decomposition
E-$(C(CH_3){=}CH_2)CHOO$ [a]	1.3	7.7×10^{-3}	Reaction with $(H_2O)_2$ and H_2O

Notes:
[a] Derived specifically from isoprene.

4. Analysis of Druett and May's "Brass tube" experiment

Based on the information given by Druett and May (1968), the gas flow through the l = 12.8 m long and d = 11.4 cm inner diameter long brass tube was 171 m^3 h^{-1} giving a gas residence time 2.75 s. The spider webs with the bacterial cells were mounted at residence times of 0, 0.8 s and 2.75 s. The slope of the exponential decay of the viable cells as a function of the operation time of the flow tube at these positions was k_{cell} = 3.3 ± 0.3, 1.6 ± 0.2, and 0.9 ± 0.7 h^{-1}, respectively. Assuming that k_{cell} is linearly related to the OAF concentration, we can estimate the first order loss rate of OAF along the brass tube from a plot of k_{cell} as a function of the residence time in the brass tube, shown in Fig. S2S4. From Fig. S2 S4 we see that the decay of bactericidal activity decreased non-exponentially, reasons for which could be manifold. First, the outdoor concentration of OAF (and its precursors) may have varied over time of operation of the flow tube. Second, the OAF is likely to be a group of individual species with variable life-times. Third, OAF may have been generated along the tube as the precursor chemistry continued. Rough values for the loss rate coefficients k_{OAF} from the first two points, the second and third points and all three combined are 0.9, 0.3 and 0.5 s^{-1}, respectively.

Model	Exponential
Equation	y = y0 + A*exp(R0*x)
Plot	B
y0	0 ± 0
A	2.86602 ± 0.61946
R0	-0.44983 ± 0.14394
Reduced Chi-Sqr	6.35626
R-Square (COD)	0.89766
Adj. R-Square	0.79532
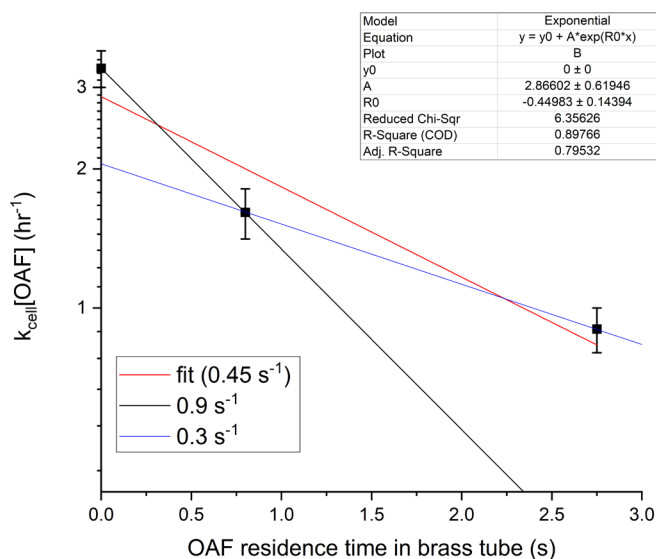
Figure S2S4: Decay of OAF driven bactericidal activity along the brass tube of the Druett and May (1968) study.

We next consider that the decreasing activity of OAF along the tube was controlled by its loss to the walls. Highly oxygenated VOC exhibit substantial partitioning to walls in tubes, via both reversible and irreversible loss processes (Deming et al., 2019). For the impact on bacterial viability over the relevant time scales, it seems that the loss was of rather of irreversible nature as reversible adsorption would have led to slow migration of the responsible species along the tube. The large flow rate implies turbulent flow conditions (Reynolds number > 30000). If we first assume perfect mixing and interaction of the agent with the wall purely driven by gas kinetics, the observed loss rate coefficient corresponds to an uptake coefficient (γ), the net, fractional efficiency (per collision) of loss from the gas-phase: γ =

$\frac{k_{OAF}d}{\omega}$, where ω is the mean thermal velocity of the OAF 'molecule'. Assuming a molecular weight between 50 and 150 g mole^{-1} and the range for k_{OAF} obtained above, γ is in the range $(1-5) \times 10^{-4}$. However, even under highly turbulent conditions, a quasi-stagnant boundary layer persists that effectively limits mass transport and could lead to an effective wall loss rate that is up to two orders of magnitude smaller (Seeley et al., 1996; Seeley et al., 1993; Donahue et al., 1996; Herndon et al., 2001). As this near-surface resistance to uptake cannot be readily assessed retrospectively for the Druett and May experiment, we conservatively conclude that the loss of OAF to the brass walls in the experiment of Druett and May is consistent with an uptake coefficient in the range of 10^{-4} to 10^{-2}.

Peroxides could fit into this range for the wall loss. For example, H_2O_2 is readily destroyed on metal and metal-oxide surfaces, for which a γ value of 1×10^{-4} has been recommended (Crowley et al., 2010). Similar uptake coefficients were observed for peracetic acid (Wu et al., 2015), and also a range of hydroperoxides from isoprene and terpene ozonolysis efficiently partition and react on or in condensed phases (Riva et al., 2017). Peroxy-radicals, with γ values ranging between 10^{-4} and 10^{-2} depending on the substrate (Ammann et al., 2013; Lakey et al., 2015; Lakey et al., 2016) also fit into this range, with higher values obtained in the presence of transition metals that may also be present in a brass tube exposed to acidifying gases. We note that the analysis of Hood (1974) did not consider the possibility that only a fraction of the collisions of the OAF with the wall may lead to its loss, which implies that the molecular weight may be overestimated so that smaller molecules and radicals considered here might remain candidates.

5. MCM Modelling of selected Dark and Nash experiments,

The chamber experiments of Dark and Nash (1970) were reanalysed using a detailed chemical model based on the present version of the Master Chemical Mechanism (MCMv3.2, http://mcm.york.ac.uk/~~http://mcm.leeds.ac.uk/MCMv3.2/~~). Simulations of reactant loss and product formation were performed for six different alkenes (propene, but-1-ene, *trans*-but-2-ene, *cis*-but-2-ene, pent-1-ene and hex-1-ene for an experiment time of 10 minutes. Initial ozone and alkene concentrations and the conditions (T =293 K and RH = 80 %) of the ozonolysis experiments were as given by Dark and Nash (1970). In total, 18 model runs were performed for the six different alkenes and the three different initial O_3 concentrations listed by Dark and Nash (1970). Concentration profiles of HO radicals, HO_2 radicals, hydrogen peroxide (H_2O_2), organic peroxides (ROOHs), aldehydes (RCHOs), alcohols (ROH), carboxylic acids (RC(O)OH) and organic peroxyl radicals (RO_2) were computed (https://chemie.tropos.de/images/Zusatzmaterial/CoxACP2021.zip). Note, groups such as RCHO contain all different aldehydes formed in the specific cases, i.e. for propene (HCHO, CH_3CHO) and for hexane (HCHO, $CH_3(CH_2)_xCHO$ with x = 0,1,2,3). Figure ~~S3~~ S5 shows the modelled data for the 11 ppbv initial ozone experiments.

To examine possible relationships between the product median concentration levels and the observed bactericidal effects, correlation coefficients and slopes between the two quantities were calculated. However, a greater slope may not necessarily imply a stronger causal relationship because of the underlying variation within the three different ozone concentrations. Similarly, owing to the small number of datapoints, statistical analyses for each specific ozone concentration revealed no clear correlation.

It is highly likely that not only the concentration but also the rate of transfer of a gas-phase product to the aqueous phase (containing the bacteria) play an important role in defining germicidal efficiency. This is manifest in the well-established principle that an efficient air-borne disinfectant must have a very low vapour pressure (Nash, 1951). For this reason, assuming that the germicidal effect of a trace-gas is proportional to its concentration and inversely proportional to p^0, we calculated the ratio (r_p) of the median concentration (expressed as a pressure) and the saturation vapour pressure (p^0) of trace gas product. Values of p^0 were taken from databases (https://chemie.tropos.de/images/Zusatzmaterial/SI_Tables_Cox_et_al.pdf), www.dguv.de/ifa/stoffdatenbank) or calculated (Compernolle et al., 2011). Values of r_p were found to increase at higher ozone conditions (i.e. higher product concentrations) and for the larger olefins.

In order to eliminate the effect of varying the ozone concentration on the relationship between the experimentally derived death fraction df (d$f = (1 - f) \cdot 100$) and r_p, the absolute differences between df and r_p for the various ozone concentrations were used; e.g. $\Delta df_{11-4} = df_{11} - df_4$ and $\Delta r_{p,11-4} = r_{p,11} - r_{p,4}$ represents the differences in both parameters for the model run with 11 and 4 ppbv ozone, respectively. In this way, the relationship of the change in the predicted product concentrations (change in the cause) to the change in the observed death fraction (change in the effect) was studied. Figure ~~S4~~ S6 shows the relationship between Δdf and Δr_p for two inorganic (HO_2, H_2O_2) and two organic (RC(O)OOH, RCHO) trace-gases. While a positive slope is generally observed, the data is very scattered and with the exception of HO_2, the correlation coefficients are < 0.5. All other trace-gases display correlations similar to that of RCHO with correlation coefficients of about 0.1.

The probability that a trace-gas partitioned to the surface region is able to penetrate through the bacterial membrane can be a key factor in determining germicidal effects. Partitioning coefficients such as the octanol-water-coefficient (K_{OW}) are often used as a proxy because the cell membrane permeability is typically linearly proportional to it (Levin et al., 1984). K_{OW} values for all oxidation products were taken from the EPIsuite database or estimated by the KOWWIN v1.67 estimation method (EPA, 2021; US-EPA, 2012). The values obtained (https://chemie.tropos.de/images/Zusatzmaterial/SI_Tables_Cox_et_al.pdf) indicate an increasing value of K_{OW} with increasing carbon chain length. From the values of K_{OW} thus obtained and the modelled concentration of each trace-gas product we calculated f_{KOW}, which is the median simulated concentration (expressed as a partial pressure) of a product multiplied by its value of K_{OW}. As for the analysis using the saturation vapour pressure, f_{KOW} was not strongly correlated with germicidal efficiency.

Possible reasons for the lack of correlation (with the exception of HO_2) between the germicidal efficiency Δdf and the Δr_p or Δf_{KOW} of a trace gas may be related to missing chemistry in the MCM mechanism used or in the assumption of a linear relationship between germicidal efficiency and either r_p or K_{OW}.
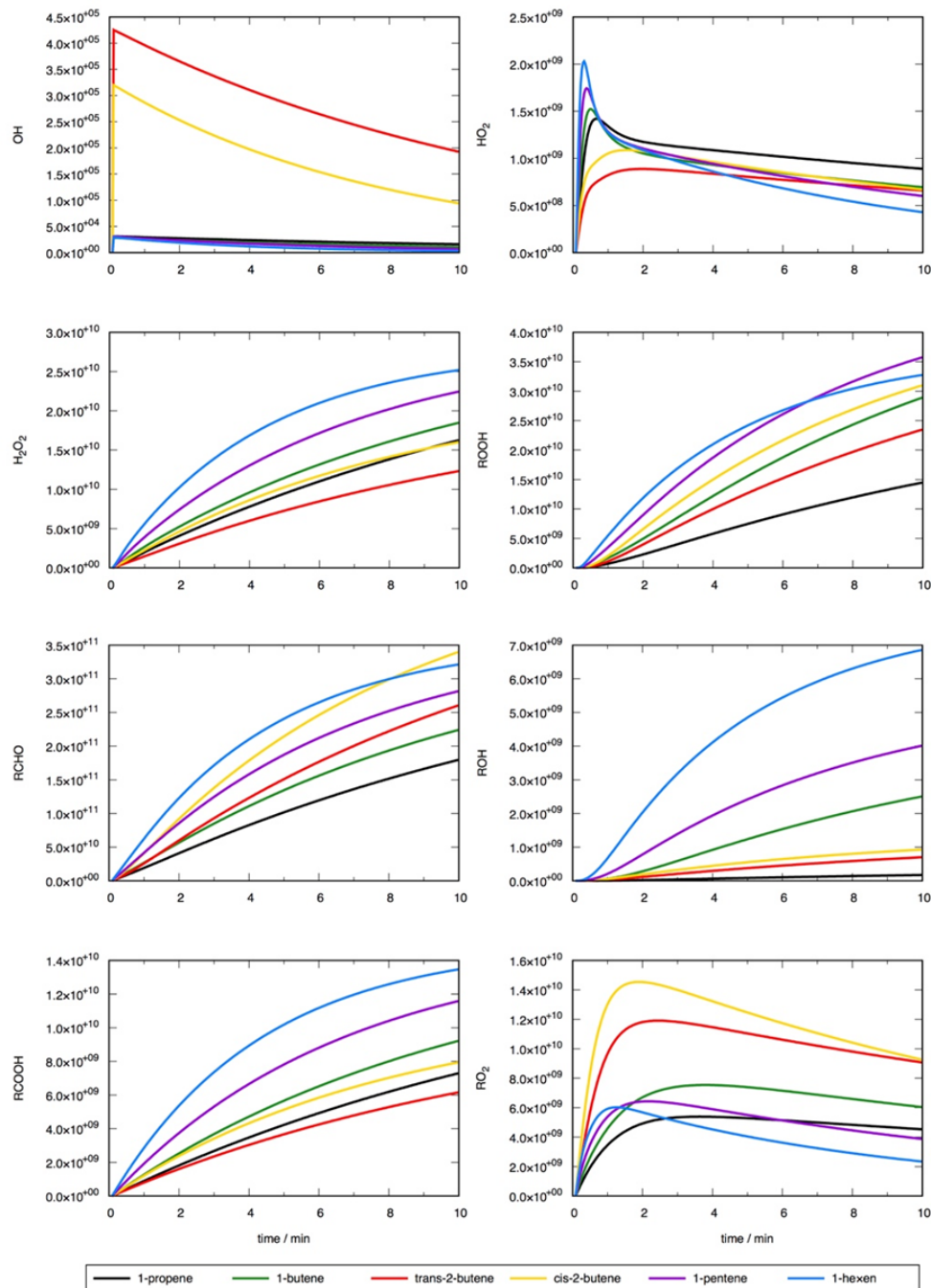
Figure S3S5: Concentration profiles for HO radicals, HO$_2$ radicals, H$_2$O$_2$, organic hydroperoxides (ROOH), aldehydes (RCHO), alcohols (ROH), carboxylic acids (ROOH), and RO$_2$ radicals in six different olefin-ozone experiments conducted by Dark and Nash (1970).

13
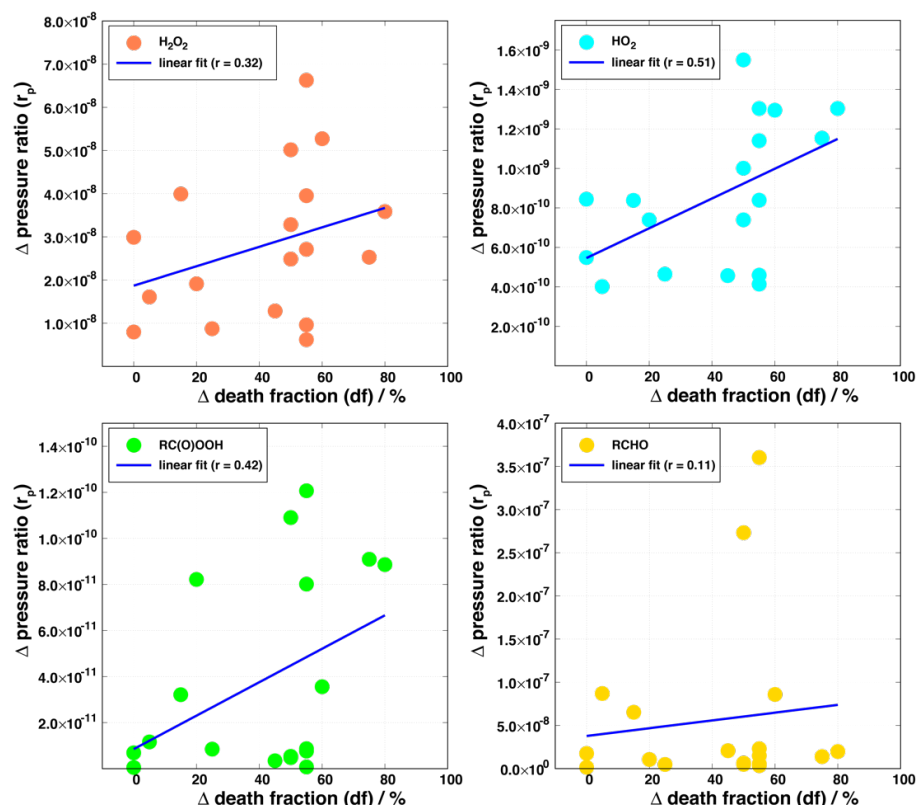
Figure ~~S4~~S6: Relationship between the absolute differences of the death fraction (df) of *Escherichia coli* and the calculated r_p ratio of the different model runs for H_2O_2, HO_2, peracids (R(O)OOH) and aldehydes (RCHO).

6. Calculations using updated alkene degradation chemistry

(a) Construction of new chemical schemes

The chemistry of small alkenes, as represented in the MCM, is currently ~~is~~ based on the rules defined by Jenkin et al. (Jenkin et al., 1997). To take account of recent advances in understanding, updated chemical schemes were constructed for the 11 alkenes shown in Fig. 1 of the main paper, the ozonolysis of which resulted in the wide range of germicidal impacts reported by Dark and Nash (Dark and Nash, 1970). Importantly, this included chemical schemes for cyclohexene and 2,4,4-trimethypent-2-ene, for which the reported impacts were at the extremes of the range, these alkenes not being treated in the MCM. The new and updated schemes represented explicitly the O_3 and HO-initiated gas-phase chemistry of the series of alkenes to first-generation products under NO_x-free conditions, with the rate coefficients for these initiation reactions taken from Cox et al. (Cox et al., 2020), Mellouki et al. (Mellouki et al., 2021, 2020) and McGillen et al. (McGillen et al., 2020). The schemes included excited Criegee intermediate (CI*) chemistry designed to recreate recommended HO and sCI yields (e.g. as reported by Cox et al. (Cox et al., 2020)), primary carbonyl yields (e.g. as summarized by Calvert et al. (Calvert et al., 2015) and Cox et al. (Cox et al., 2020)), and reported yields of other products formed from the prompt decomposition of CI* (e.g. HO_2, ketenes, etc.), where available, e.g. Tuazon et al. (Tuazon et al., 1997) for propene, *cis*-but-2-ene, *trans*-but-2-ene and 2-methybut-2-ene; Aschmann et al. (Aschmann et al., 2003) and Hansel et al. (Hansel et al., 2018) for cyclohexene.

14

The sCI chemistry was based on, or inferred from the recommendations of Cox et al. (2020) and the theoretical/structure-activity relationship (SAR) methods of Vereecken et al. (Vereecken et al., 2017). This includes unimolecular decomposition (e.g. to form HO and organic radical co-products), reaction with H_2O and $(H_2O)_2$, and reaction with the primary carbonyl and carboxylic acid products formed in each alkene system to form secondary ozonides and hydroperoxy-esters.

The bimolecular reactions of peroxy (RO_2) radicals formed from the O_3 and HO-initiated chemistry was based on the recommendations of Jenkin et al. (Jenkin et al., 2019), with a parameterized representation of RO_2 permutation reactions. In the specific case of the complex C_6 RO_2 radicals formed from cyclohexene oxidation, unimolecular isomerization reactions were included, based on the methods of Vereecken and Nozière (Vereecken and Nozière, 2020), allowing rapid formation of HOMs via the resultant autooxidation mechanism, and the formation of the main series of products reported by Aschmann et al. (Aschmann et al., 2003) and Hansel et al. (Hansel et al., 2018). Where appropriate, the decomposition and isomerization chemistry of the oxy (RO) radicals formed in the various systems was based on the methods of Vereecken and Peeters (Vereecken and Peeters, 2010, 2009). The new mechanisms are listed in Table S4, along with a key to species identity in Table S5.

(b) Results

Simulations of the 11 alkene systems were carried out for each of the three ozone regimes for the 10 minute experiment duration, using the initial conditions reported by Dark and Nash (1970). The average gas-phase concentrations of a series of products or product classes were plotted against the average *E. coli* loss rates (k_{loss}) summarised in Table S1. The products included sCIs, the radical species HO, HO_2 and RO_2, and the closed-shell products, RCHO, RC(O)R, H_2O_2, ROOH, RC(O)OOH, RC(O)OH, ketenes and secondary ozonides. No clear correlations were observed for any product, as shown in Figs. S7 and S8. Figure 2a of the main text also shows example results for species containing -OOH groups (including H_2O_2, ROOH, ~~and~~ RC(O)OOH and total -OOH) ~~and Fig. S5 the results for RCHO~~ for the 33 ppb ozone experiments, showing that ~~In each case,~~ the concentrations of -OOH species generated from alkenes with low (or zero) germicidal impacts (2-methylbut-2-ene and 2,4,4-trimethylpent-2-ene) are comparable with those generated from cyclohexene, which has the highest germicidal impact.

It is noted, however, that the broad product classes formed in the various systems can include a structurally diverse set of compounds, which may possess different propensities to penetrate the protective membrane of the microorganisms and initiate oxidation. Peroxidic compounds such as H_2O_2 and peracetic acid ($CH_3C(O)OOH$) are known germicides (e.g. (McDonnell and Russell, 1999)), and the speciation was considered in more detail. Figure 2b,c,d of the main text and Fig. S9 shows the simulated speciation of peroxidic compounds generated from the ozonolysis of 2-methylbut-2-ene, 2,4,4-trimethylpent-2-ene and cyclohexene (33 ppb ozone experiments). For 2-methylbut-2-ene and 2,4,4-trimethylpent-2-ene, the most important contributors are the β-hydroxy species formed from secondary attack of HO on the parent alkenes (accounting of 75 % and 63 % of the peroxide burden, respectively) with additional contributions resulting mainly from the chemistry of the organic co-radical(s) formed with HO from the ozonolysis mechanism (e.g. $CH_3C(O)CH_2OOH$, $CH_3C(O)OOH$ and CH_3OOH from the chemistry of $CH_3C(O)CH_2$ co-radical, and $HC(O)CH_2OOH$ from the chemistry of $HC(O)CH_2$ co-radical in the 2-methylbut-2-ene system). As a

result, the peroxide concentrations for the complete series of acyclic alkenes (Fig. S3) broadly follow the trend in HO yields, with underlying contributions from α-hydroxy ROOH and H_2O_2 formed from the reactions of some sCIs with H_2O and $(H_2O)_2$. In the case of cyclohexene, however, important additional contributions result from autooxidation chemistry involving peroxy radicals formed from the organic co-radical, $HC(O)CH_2CH_2CH_2CHCHO$. This leads to additional rapid formation of a number of multi-functional species (HOMs) containing -OOH and -C(O)OOH groups, resulting from sequential H-shift isomerisation reactions, as also reported experimentally (e.g. Hansel et al., 2018). It is probable that such multifunctional species may show an increased propensity for uptake to surfaces. In contrast, it is noted that the majority of hydroperoxide species formed from 2-methylbut-2-ene and 2,4,4-trimethylpent-2-ene are either tertiary and/or contain bulky β-substituents which may have an influence on uptake and/or the decomposition rates and pathways in the condensed phase. Clearly further work is required on the structural dependence of germicidal properties of hydroperoxides and other oxygenated products of alkene ozonolysis.
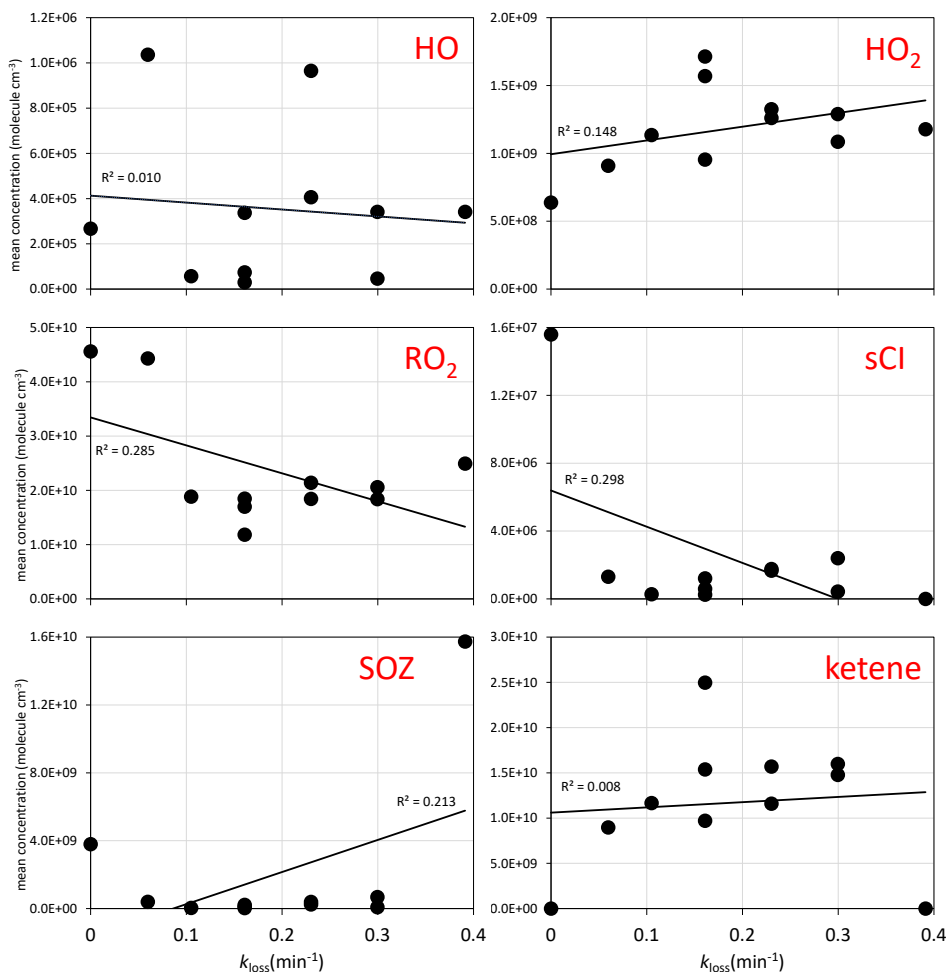
Figure S7: Simulated concentrations of HO, HO_2, RO_2, sCI, secondary ozonide (SOZ) and ketene products vs. k_{loss} for *E. coli* in 33 ppb O_3 experiments for the series of 11 alkenes shown in Fig. 1 of the main paper; and linear regression of the data.

16
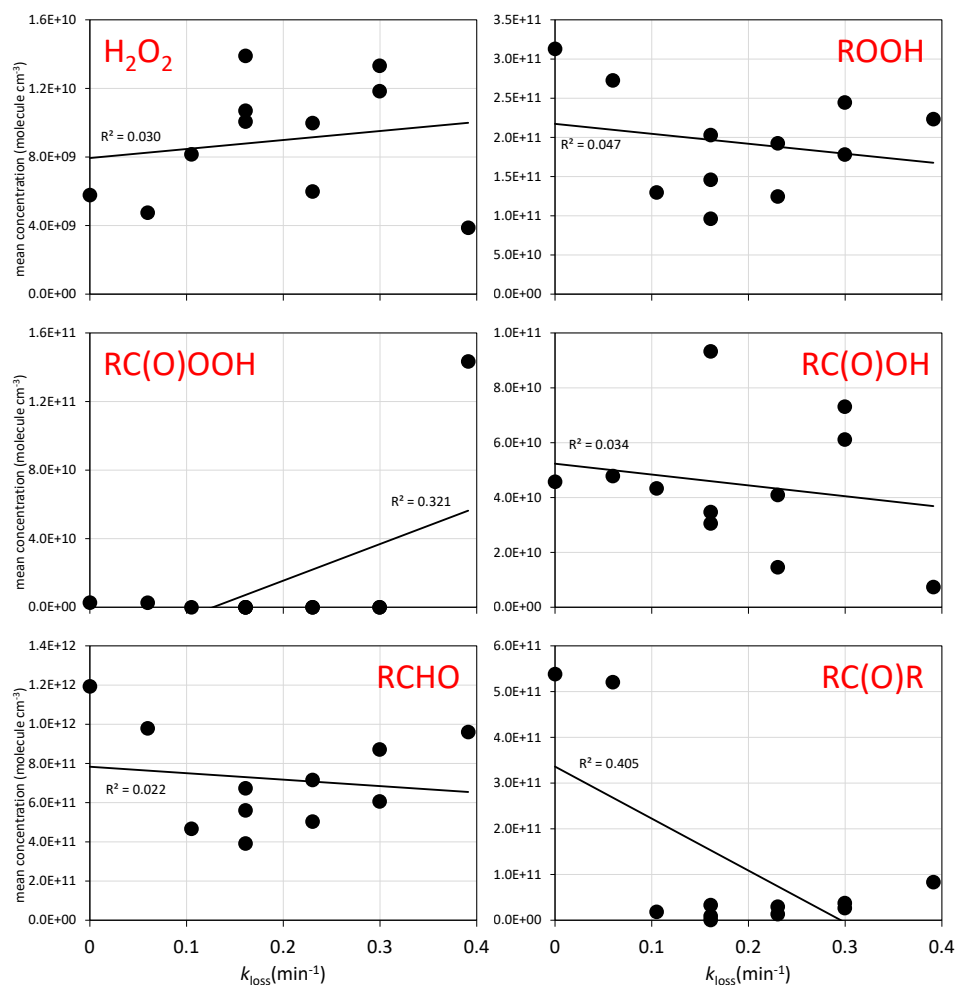
Figure S8: Simulated concentrations of H_2O_2, ROOH, RC(O)OOH, RC(O)OH, RCHO and RC(O)R products vs. k_{loss} for *E. coli* in 33 ppb O_3 experiments for the series of 11 alkenes shown in Fig. 1 of the main paper; and linear regression of the data.
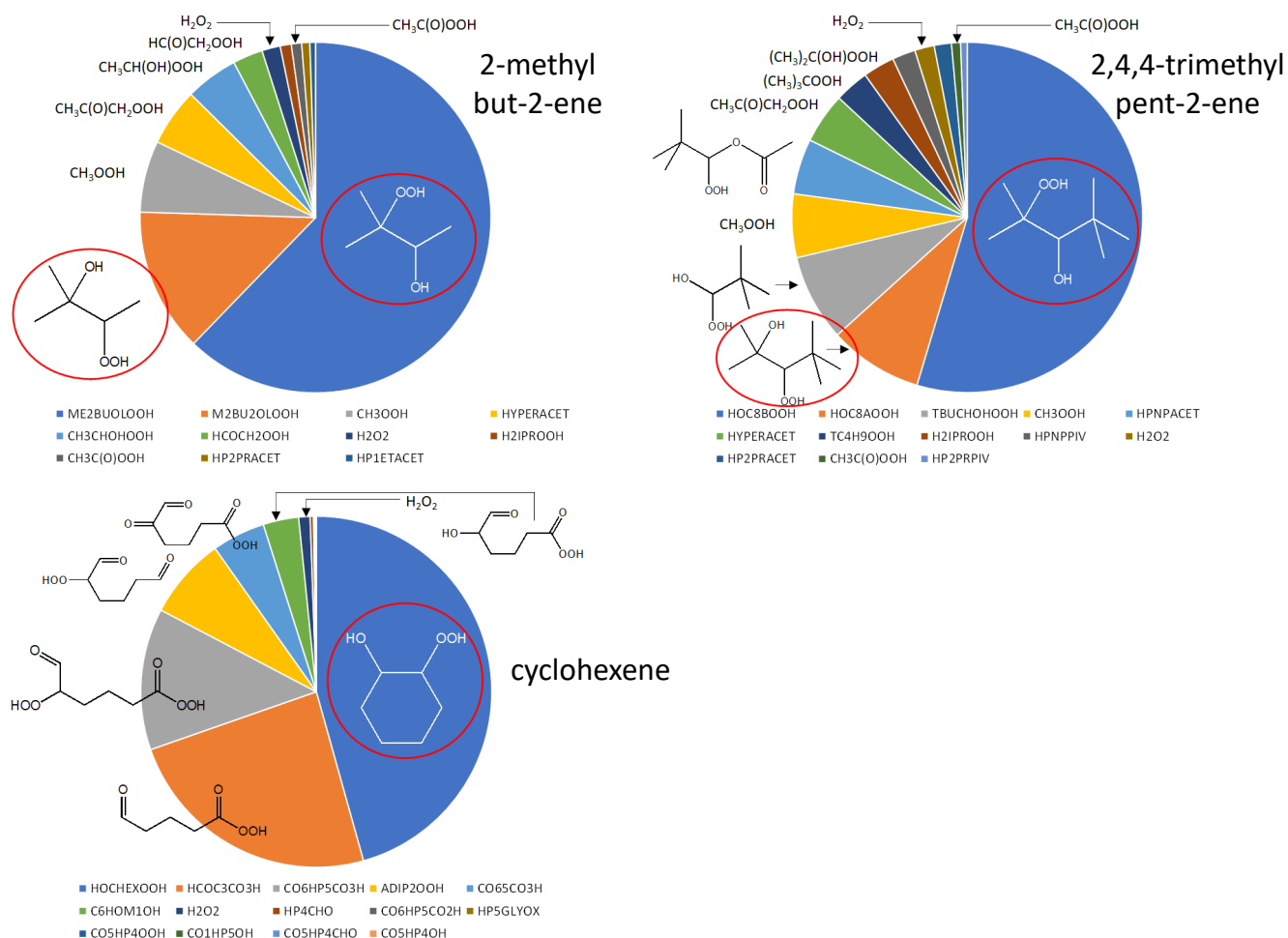
Figure S9. Simulated speciation of peroxidic compounds generated from 2-methylbut-2-ene, 2,4,4-trimethylpent-2-ene and cyclohexene in the 33 ppb O_3 experiments. The total -OOH concentrations in the three cases were 2.8×10^{11}, 3.2×10^{11} and 3.7×10^{11} molecule cm^{-3}. Species in red ellipses are those formed from the HO + alkene reactions. A key to species identity is given in Table S5.

(c) Uncertainties

Mechanistic uncertainties: The new chemical schemes are designed to incorporate up-to-date kinetic and mechanistic information, as described above. Despite this, there are remaining uncertainties in the chemistry of alkene ozonolysis, as discussed in recent reviews, e.g., Osborn and Taatjes (2015); Vereecken et al. (2017); Khan et al. (2018); Cox et al. (2020); Caravan et al. (2021). A particular area of uncertainty for the current study is the product distribution formed from the reactions of sCIs with H_2O and $(H_2O)_2$. As illustrated above in section 3c, these reactions are major atmospheric loss routes for CH_2OO and generally for *E*- mono-substituted sCIs, and they are also important loss routes for the conditions of the Dark and Nash (1970) experiments. The product channel contributions have only been fully characterized for the reactions of CH_2OO with H_2O (Nguyen et al., 2016) and $(H_2O)_2$ (Nguyen et al., 2016; Sheps et al., 2017). Although both these studies report significant formation of the α-hydroxy hydroperoxide product, $HOCH_2OOH$, for the $(H_2O)_2$ reaction (40% and 55%, respectively), there is substantial disagreement on the

18

importance of the channels forming HCHO + H_2O_2 (6% and 40%) and HC(O)OH (54% and <10%), and IUPAC currently makes no recommendations for the product channel branching ratios for either the H_2O or $(H_2O)_2$ reaction (Cox et al., 2020). In the present work, we have adopted the product channels reported by Nguyen et al. (2016), because they report branching ratios for both reactions under chamber conditions. Furthermore, the same product channel contributions are applied to all sCIs by analogy, in the absence of reported information, and this assumption could mask any trends in the formation of H_2O_2, α-hydroxy hydroperoxides and carboxylic acids from these sources. Clearly, additional studies are required to reduce uncertainty in this area and to identify any systematic dependences in the branching ratios from one sCI to another.

As indicated above, the mechanisms also include the formation of secondary ozonides from the reactions of sCIs with the primary carbonyl products formed in each alkene system. The results show that the gas phase formation of secondary ozonides (SOZs) is unimportant for most of the alkene systems considered (see Fig. S7). This is because removal of the stabilized Criegee intermediates (sCIs) formed is generally dominated by either thermal decomposition or reaction with H_2O and $(H_2O)_2$, thereby precluding significant formation of SOZs from their secondary reactions with the product aldehydes or ketones. The only exceptions are the 2,4,4-trimethylpent-2-ene and cyclohexene systems, which have the lowest and highest germicidal impacts of the alkene systems considered. In the former case, both thermal decomposition and reaction with H_2O and $(H_2O)_2$ are predicted to be relatively slow for one sCI (Z-pivaldehyde oxide, Z-$(CH_3)_3$CCHOO) (Vereecken et al., 2017), allowing its reaction with the product pivaldehyde (in particular) to compete to some extent, forming a C_{10} SOZ (about 150 ppt in the 33 ppb ozone experiment).

In the case of cyclohexene, the small yield (3 %) of the *E*- and *Z*- carbonyl-substituted sCIs is represented to react exclusively by ring-closure to form an SOZ, this being based on the extremely rapid rate coefficients calculated by Long et al. (2019). This results in about 600 ppt SOZ in the 33 ppb ozone experiment (see Fig. S7). However, it is noted that Berndt et al. (2017) reported detection of the cyclohexene-derived carbonyl-substituted sCI(s), and tentative rate coefficients for the bimolecular reactions with added SO_2, acetone and acetic acid – suggesting that rapid SOZ formation does not occur. Either way, the trend of gas-phase SOZ formation for the series of alkenes considered cannot explain the variation of germicidal impact observed by Dark and Nash (1970), although further work is required to establish the extent of intramolecular SOZ formation from small cyclic alkenes with low sCI yields. We note that, in some contrast, in the condensed phase, typical fates of the sCI are 1,3-dipolar cycloaddition with the carbonyl containing product that was formed from the decomposition of the primary ozonide (Zahardis and Petrucci, 2007). The products of these reactions are SOZ or polymeric ozonides. Cycloaddition with another sCI leads to diperoxides and peroxidic polymers. In presence of protic solvents, hydroperoxides are formed (Bailey, 1958). Thus, the formation of SOZ is strongly depending on the polarity of the condensed-phase matrix. As already mentioned in the submitted manuscript, the germicidal effects of ozonized unsaturated oils were suggested to be related to the presence of SOZ (Travagli et al., 2010). But since the alkenes considered as OAF precursors in the Dark and Nash (1970) work are not being oxidised to an appreciable degree in the condensed phase, condensed phase SOZ are not relevant there. In addition, since peroxides generally contribute to the health impact of particulate matter, it is important that any potential direct health effects of airborne germicides contributing to the OAF are also identified and investigated.

Mechanistic simplifications: The schemes written here also contain some simplifications, the possible effects of which were assessed. The HO-initiated chemistry takes account of the major product channels resulting from HO addition to the C=C bonds but, for expediency, omits the minor channels resulting from H atom abstraction from the substituent groups. These are estimated to account for between 1% and 22% of the reaction for the series of alkenes (8% on average), based on the structure-activity relationship methods of Jenkin et al. (2018), being systematically more important for cyclohexene and the larger acyclic alkenes. These reactions would tend to generate unsaturated mono-functional oxygenated products, in particular alk-1-enyl oxygenates (e.g., allyl hydroperoxide and acrolein in the case of the simplest alkene, propene), in place of the corresponding β-hydroxy substituted product classes formed from the HO addition chemistry. In addition, unimolecular ring-closure reactions might be operative for some of the unsaturated RO_2 formed (Vereecken et al., 2021), potentially providing minor routes to highly oxygenated products. A broad assessment of the trend in formation of such unsaturated and highly oxygenated products was carried out (based on HO yields of the O_3 + alkene reactions and the H atom abstraction fractions), but there was no correlation with the reported germicidal impacts reported by Dark and Nash (1970) (Table S1), largely reflecting that the impacts do not correlate with alkene size.

For simplicity, the schemes applied here also use a parameterized representation of the RO_2 permutation reactions (i.e., $RO_2 + RO_2$ and $RO_2 + R'O_2$) in which each RO_2 reacts with the pool of peroxy radicals in a pseudo-unimolecular reaction (Jenkin et al., 2019), as shown in Table S4. As a result, it was not possible to represent the product channels forming ROOR (or ROOR') + O_2, because part of the ROOR/ROOR' product derives from the peroxy radical pool rather than from the reacting RO_2 (see discussion in Jenkin et al., 2019). In practice, the contributions of these channels, and their dependence on peroxy radical structure, are not generally well characterized, and even an explicit representation of the reactions would therefore have substantial uncertainties associated with the yields of these products. However, assuming only a modest structural dependence, their collective formation efficiency might be expected to be mainly governed by the peroxy radical concentration which, as indicated above and shown in Fig. S7, shows no correlation with the reported germicidal impacts.

Potential impact of impurity NOx: Finally, the analysis we have carried out assumes that the Dark and Nash (1970) experiments were carried out under NO_x-free conditions. Their chamber experiments were nominally carried out in the absence of NO (which could otherwise have a provided a major reaction partner for the peroxy radicals, RO_2 and HO_2) and alkene impurities, and they report a systematic procedure for minimizing the impacts of such impurities. However, their procedure would result in any NO_x present being in the form of NO_2 rather than NO, and we therefore cannot rule out the possibility of trace levels of NO_2 being present in their experiments. Peroxy radicals also react with NO_2, but the impact of these reactions is limited in the majority of cases because the product peroxy-nitrates (RO_2NO_2) are generally thermally unstable, decomposing rapidly to regenerate RO_2 and NO_2. Based on the generic rate coefficients recommended by Jenkin et al. (2019), this occurs on the timescale of about 200 ms for a typical RO_2NO_2 (298 K, 760 Torr). As a result, an approximately unchanged steady state concentration of RO_2 is rapidly established, with RO_2NO_2 present at about 4 % of the RO_2 concentration at an example level of 1 ppb NO_2 (and systematically higher at higher levels of NO_2). In the specific cases of acyl peroxy radicals ($RC(O)O_2$), however, the product peroxy-acyl nitrates (PANs) are effectively stable species on the experimental timescale, and the presence of NO_2 could inhibit

20

the formation of products from their alternative reaction pathways, including peroxy acids (RC(O)OOH) formed from the reactions with HO_2 or by unimolecular isomerization. For the linear alkene systems considered, acyl peroxy radicals are not formed from the first-generation ozonolysis chemistry, and no significant effect of trace levels of NO_2 would be expected. In the cases of cyclohexene (at the high end of the germicidal impact range), and to a lesser extent 2-methylbut-2-ene and 2,4,4-trimethylpent-2-ene (at the low end of the germicidal impact range), however, acyl peroxy radicals are formed from the first-generation chemistry. As shown in Fig. S8, significant formation of RC(O)OOH is simulated to occur in these systems under NO_x-free conditions, particularly for cyclohexene (the mean concentrations are about 1.4×10^{11} molecule cm^{-3} for cyclohexene, and about 2.7×10^9 molecule cm^{-3} for each of 2-methylbut-2-ene and 2,4,4-trimethylpent-2-ene). Reaction of $RC(O)O_2$ with ≥ 1 ppb NO_2 can generally compete with the other bimolecular reactions for $RC(O)O_2$ (i.e., with HO_2 and RO_2) and would therefore have an impact on the formation of RC(O)OOH and other bimolecular reaction products. In the particularly important case of cyclohexene, however, a significant proportion of the RC(O)OOH (and other -OOH species) is formed from the auto-oxidation chemistry, involving peroxy radical isomerization reactions. These reactions are generally sufficiently rapid that the presence of ppb levels of NO_2 is predicted to have a reduced effect compared with its impact on the bimolecular reaction products. It is also noted that when the corresponding PANs may be formed, they are generally multifunctional species also containing -OOH groups. Whilst these considerations of the possible effects of NO_x are important, they do not allow any further insight into the likely identity (or identities) of the germicidal agent responsible for the open-air factor. Highly-instrumented chamber studies would be valuable to help relate germicidal impacts systematically to particular classes of reaction product formed in simulated atmospheric systems.

Table S4: Updated chemical schemes for the 11 alkenes shown in Fig. 1 of the main paper. A key to species identity is provided in Table S5.[a]

Rate coefficient [b]	Reaction
Propene	
O_3 initiation reactions	
5.77E-15*EXP(-1880/T)*0.35	O3 + C3H6 = CH2OOA + CH3CHO
5.77E-15*EXP(-1880/T)*0.32	O3 + C3H6 = ZCH3CHOOA + HCHO
5.77E-15*EXP(-1880/T)*0.33	O3 + C3H6 = ECH3CHOOA + HCHO
Excited CI chemistry	
KDEC*0.6 [c]	CH2OOA = CH2OO
KDEC*0.118	CH2OOA = CO + HO2 + OH
KDEC*0.124	CH2OOA = CO
KDEC*0.124	CH2OOA = H2
KDEC*0.034	CH2OOA = HO2 + HO2
KDEC*0.13	ZCH3CHOOA = ZCH3CHOO
KDEC*0.87	ZCH3CHOOA = HCOCH2O2 + OH
KDEC*0.13	ECH3CHOOA = ECH3CHOO
KDEC*0.334	ECH3CHOOA = CH4
KDEC*0.192	ECH3CHOOA = CH3OH + CO
KDEC*0.125	ECH3CHOOA = CH2CO
KDEC*0.219	ECH3CHOOA = CH3O2 + HO2
Stabilized sCI chemistry	
2.8E-16*[H₂O]*0.73	CH2OO = HOCH2OOH
2.8E-16*[H₂O]*0.06	CH2OO = HCHO + H2O2
2.8E-16*[H₂O]*0.21	CH2OO = HCOOH
7.35E-18*EXP(4076/T)*[(H₂O)₂]*0.40	CH2OO = HOCH2OOH
7.35E-18*EXP(4076/T)*[(H₂O)₂]*0.06	CH2OO = HCHO + H2O2
7.35E-18*EXP(4076/T)*[(H₂O)₂]*0.54	CH2OO = HCOOH
1.52E-11*EXP(590/T)	CH2OO + HCOOH = HPMEFORM
1.30E-10	CH2OO + CH3CO2H = HPMEACET
1.70E-12	CH2OO + HCHO = CSOZC
1.70E-12	CH2OO + CH3CHO = C2SOZC
7.4E+6*EXP(-3220/T)	ZCH3CHOO = HCOCH2O2 + OH
6.84E-19*[H₂O]*0.73	ZCH3CHOO = CH3CHOHOOH
6.84E-19*[H₂O]*0.06	ZCH3CHOO = CH3CHO + H2O2

6.84E-19*[H$_2$O]*0.21	ZCH3CHOO = CH3CO2H
2.05E-15*[(H$_2$O)$_2$]*0.40	ZCH3CHOO = CH3CHOHOOH
2.05E-15*[(H$_2$O)$_2$]*0.06	ZCH3CHOO = CH3CHO + H2O2
2.05E-15*[(H$_2$O)$_2$]*0.54	ZCH3CHOO = CH3CO2H
2.50E-10	ZCH3CHOO + HCOOH = HP1ETFORM
1.70E-10	ZCH3CHOO + CH3CO2H = HP1ETACET
1.70E-12	ZCH3CHOO + HCHO = C2SOZC
1.70E-12	ZCH3CHOO + CH3CHO = C2SOZC2
1.94E+09*T$^{1.35}$*EXP(-7445/T)	ECH3CHOO = CH3CO2H
1.3E-14*[H$_2$O]*0.73	ECH3CHOO = CH3CHOHOOH
1.3E-14*[H$_2$O]*0.06	ECH3CHOO = CH3CHO + H2O2
1.3E-14*[H$_2$O]*0.21	ECH3CHOO = CH3CO2H
4.4E-11*[(H$_2$O)$_2$]*0.40	ECH3CHOO = CH3CHOHOOH
4.4E-11*[(H$_2$O)$_2$]*0.06	ECH3CHOO = CH3CHO + H2O2
4.4E-11*[(H$_2$O)$_2$]*0.54	ECH3CHOO = CH3CO2H
5.00E-10	ECH3CHOO + HCOOH = HP1ETFORM
2.50E-10	ECH3CHOO + CH3CO2H = HP1ETACET
1.70E-12	ECH3CHOO + HCHO = C2SOZC
1.70E-12	ECH3CHOO + CH3CHO = C2SOZC2
OH initiation reactions	
KMT16*0.137 [d]	OH + C3H6 = HYPROPO2
KMT16*0.863	OH + C3H6 = IPROPOLO2
RO$_2$ and RO chemistry	
KRO2HO2*0.498*0.82 [e]	HCOCH2O2 + HO2 = HCOCH2OOH
KRO2HO2*0.498*0.18	HCOCH2O2 + HO2 = HCOCH2O + OH
1.00E-13*EXP(974/T)*0.2*[RO$_2$] [f]	HCOCH2O2 = GLYOX
1.00E-13*EXP(974/T)*0.6*[RO$_2$]	HCOCH2O2 = HCOCH2O
1.00E-13*EXP(974/T)*0.2*[RO$_2$]	HCOCH2O2 = HOCH2CHO
KDEC	HCOCH2O = HCHO + CO + HO2
3.8E-13*EXP(780/T)*(1-1/(1+498*EXP(-1160/T)))	CH3O2 + HO2 = CH3OOH
3.8E-13*EXP(780/T)*(1/(1+498*EXP(-1160/T)))	CH3O2 + HO2 = HCHO
2.06E-13*EXP(365/T)*7.2*EXP(-885/T)*[RO$_2$]	CH3O2 = CH3O
1.03E-13*EXP(365/T)*(1-7.2*EXP(-885/T))*[RO$_2$]	CH3O2 = CH3OH
1.03E-13*EXP(365/T)*(1-7.2*EXP(-885/T))*[RO$_2$]	CH3O2 = HCHO
7.2E-14*EXP(-1080/T)*[O$_2$]	CH3O = HCHO + HO2

KRO2HO2*0.601	HYPROPO2 + HO2 = HYPROPO2H
1.00E-13*EXP(570/T)*0.2*[RO$_2$]	HYPROPO2 = ACETOL
1.00E-13*EXP(570/T)*0.6*[RO$_2$]	HYPROPO2 = HYPROPO
1.00E-13*EXP(570/T)*0.2*[RO$_2$]	HYPROPO2 = PROPGLY
2.00E+14*EXP(-6410/T)	HYPROPO = CH3CHO + HCHO + HO2
KRO2HO2*0.601	IPROPOLO2 + HO2 = IPROPOLO2H
1.00E-13*EXP(942/T)*0.2*[RO$_2$]	IPROPOLO2 = CH3CHOHCHO
1.00E-13*EXP(942/T)*0.6*[RO$_2$]	IPROPOLO2 = IPROPOLO
1.00E-13*EXP(942/T)*0.2*[RO$_2$]	IPROPOLO2 = PROPGLY
2.00E+14*EXP(-5505/T)	IPROPOLO = CH3CHO + HCHO + HO2
But-1-ene	
O$_3$ initiation reactions	
3.55E-15*EXP(-1750/T)*0.35	O3 + BUT1ENE = CH2OOB + C2H5CHO
3.55E-15*EXP(-1750/T)*0.325	O3 + BUT1ENE = ZC2H5CHOOA + HCHO
3.55E-15*EXP(-1750/T)*0.325	O3 + BUT1ENE = EC2H5CHOOA + HCHO
Excited CI chemistry	
KDEC*0.7	CH2OOB = CH2OO
KDEC*0.088	CH2OOB = CO + HO2 + OH
KDEC*0.093	CH2OOB = CO
KDEC*0.093	CH2OOB = H2
KDEC*0.026	CH2OOB = HO2 + HO2
KDEC*0.15	ZC2H5CHOOA = ZC2H5CHOO
KDEC*0.85	ZC2H5CHOOA = PROPALO2 + OH
KDEC*0.15	EC2H5CHOOA = EC2H5CHOO
KDEC*0.326	EC2H5CHOOA = C2H6
KDEC*0.188	EC2H5CHOOA = C2H5OH + CO
KDEC*0.122	EC2H5CHOOA = CH3CHCO
KDEC*0.214	EC2H5CHOOA = C2H5O2 + HO2
Stabilized sCI chemistry	
1.30E-10	CH2OO + PROPACID = HPMEPROP
1.70E-12	CH2OO + C2H5CHO = C3SOZC
2.41E-62*T$^{24.33}$*EXP(2571/T)	ZC2H5CHOO = PROPALO2 + OH
1.51E-18*[H$_2$O]*0.73	ZC2H5CHOO = ETCHOHOOH
1.51E-18*[H$_2$O]*0.06	ZC2H5CHOO = C2H5CHO + H2O2
1.51E-18*[H$_2$O]*0.21	ZC2H5CHOO = PROPACID

4.31E-15*[(H$_2$O)$_2$]*0.40	ZC2H5CHOO = ETCHOHOOH
4.31E-15*[(H$_2$O)$_2$]*0.06	ZC2H5CHOO = C2H5CHO + H2O2
4.31E-15*[(H$_2$O)$_2$]*0.54	ZC2H5CHOO = PROPACID
2.50E-10	ZC2H5CHOO + HCOOH = HP1PRFORM
1.70E-10	ZC2H5CHOO + PROPACID = HP1PRPROP
1.70E-12	ZC2H5CHOO + HCHO = C3SOZC
1.70E-12	ZC2H5CHOO + C2H5CHO = C3SOZC3
1.57E10*T$^{1.03}$*EXP(-7464/T)	EC2H5CHOO = PROPACID
1.58E-14*[H$_2$O]*0.73	EC2H5CHOO = ETCHOHOOH
1.58E-14*[H$_2$O]*0.06	EC2H5CHOO = C2H5CHO + H2O2
1.58E-14*[H$_2$O]*0.21	EC2H5CHOO = PROPACID
1.75E-11*[(H$_2$O)$_2$]*0.40	EC2H5CHOO = ETCHOHOOH
1.75E-11*[(H$_2$O)$_2$]*0.06	EC2H5CHOO = C2H5CHO + H2O2
1.75E-11*[(H$_2$O)$_2$]*0.54	EC2H5CHOO = PROPACID
5.00E-10	EC2H5CHOO + HCOOH = HP1PRFORM
2.50E-10	EC2H5CHOO + PROPACID = HP1PRPROP
1.70E-12	EC2H5CHOO + HCHO = C3SOZC
1.70E-12	EC2H5CHOO + C2H5CHO = C3SOZC3
OH initiation reactions	
6.6E-12*EXP(465/T)*0.137	BUT1ENE + OH = HO3C4O2
6.6E-12*EXP(465/T)*0.863	BUT1ENE + OH = NBUTOLAO2
RO$_2$ and RO chemistry	
6.4E-13*EXP(710/T)	C2H5O2 + HO2 = C2H5OOH
1.00E-13*EXP(353/T)*0.6*[RO$_2$]	C2H5O2 = C2H5O
1.00E-13*EXP(353/T)*0.2*[RO$_2$]	C2H5O2 = C2H5OH
1.00E-13*EXP(353/T)*0.2*[RO$_2$]	C2H5O2 = CH3CHO
2.4E-14*EXP(-325/T)*[O$_2$]	C2H5O = CH3CHO + HO2
KRO2HO2*0.601*0.82	PROPALO2 + HO2 = PROPALOOH
KRO2HO2*0.601*0.18	PROPALO2 + HO2 = PROPALO + OH
1.00E-13*EXP(674/T)*0.2*[RO$_2$]	PROPALO2 = CH3CHOHCHO
1.00E-13*EXP(674/T)*0.2*[RO$_2$]	PROPALO2 = MGLYOX
1.00E-13*EXP(674/T)*0.6*[RO$_2$]	PROPALO2 = PROPALO
KDEC	PROPALO = CH3CHO + HO2 + CO
KRO2HO2*0.683	HO3C4O2 + HO2 = HO3C4OOH
1.00E-13*EXP(983/T)*0.2*[RO$_2$]	HO3C4O2 = HO3C3CHO

1.00E-13*EXP(983/T)*0.6*[RO$_2$]	HO3C4O2 = HO3C4O
1.00E-13*EXP(983/T)*0.2*[RO$_2$]	HO3C4O2 = NBUTOLAOH
1.80E+13*EXP(-5234/T)	HO3C4O = C2H5CHO + HCHO + HO2
1.20E+11*EXP(-3825/T)	HO3C4O = HO34C4O2
KRO2HO2*0.683	NBUTOLAO2 + HO2 = NBUTOLAOOH
1.00E-13*EXP(675/T)*0.2*[RO$_2$]	NBUTOLAO2 = MEKCOH
1.00E-13*EXP(675/T)*0.6*[RO$_2$]	NBUTOLAO2 = NBUTOLAO
1.00E-13*EXP(675/T)*0.2*[RO$_2$]	NBUTOLAO2 = NBUTOLAOH
2.00E+14*EXP(-6354/T)	NBUTOLAO = C2H5CHO + HCHO + HO2
KRO2HO2*0.748	HO34C4O2 + HO2 = HO34C4OOH
1.00E-13*EXP(785/T)*0.2*[RO$_2$]	HO34C4O2 = HO34C3CHO
1.00E-13*EXP(785/T)*0.6*[RO$_2$]	HO34C4O2 = HO34C4O
1.00E-13*EXP(785/T)*0.2*[RO$_2$]	HO34C4O2 = HO13C4OH
8.00E+10*EXP(-2417/T)	HO34C4O = HO13C3CHO + HO2
Pent-1-ene	
O$_3$ initiation reactions	
2.13E-15*EXP(-1580/T)*0.35	PENT1ENE + O3 = CH2OOC + C3H7CHO
2.13E-15*EXP(-1580/T)*0.325	PENT1ENE + O3 = ZC3H7CHOOA + HCHO
2.13E-15*EXP(-1580/T)*0.325	PENT1ENE + O3 = EC3H7CHOOA + HCHO
Excited CI chemistry	
KDEC*0.9	CH2OOC = CH2OO
KDEC*0.029	CH2OOC = CO + HO2 + OH
KDEC*0.031	CH2OOC = CO
KDEC*0.031	CH2OOC = H2
KDEC*0.009	CH2OOC = HO2 + HO2
KDEC*0.19	ZC3H7CHOOA = ZC3H7CHOO
KDEC*0.81	ZC3H7CHOOA = BUTALAO2 + OH
KDEC*0.19	EC3H7CHOOA = EC3H7CHOO
KDEC*0.311	EC3H7CHOOA = C3H8
KDEC*0.179	EC3H7CHOOA = NPROPOL + CO
KDEC*0.116	EC3H7CHOOA = C2H5CHCO
KDEC*0.204	EC3H7CHOOA = NC3H7O2 + HO2
Stabilized sCI chemistry	
1.30E-10	CH2OO + BUTACID = HPMEBUTR
1.70E-12	CH2OO + C3H7CHO = C4SOZC

$2.41E-62*T^{24.33}*EXP(2571/T)$	ZC3H7CHOO = BUTALAO2 + OH
$1.51E-18*[H_2O]*0.73$	ZC3H7CHOO = PRCHOHOOH
$1.51E-18*[H_2O]*0.06$	ZC3H7CHOO = C3H7CHO + H2O2
$1.51E-18*[H_2O]*0.21$	ZC3H7CHOO = BUTACID
$4.31E-15*[(H_2O)_2]*0.40$	ZC3H7CHOO = PRCHOHOOH
$4.31E-15*[(H_2O)_2]*0.06$	ZC3H7CHOO = C3H7CHO + H2O2
$4.31E-15*[(H_2O)_2]*0.54$	ZC2H5CHOO = BUTACID
2.50E-10	ZC3H7CHOO + HCOOH = HP1BUFORM
1.70E-10	ZC3H7CHOO + BUTACID = HP1BUBUTR
1.70E-12	ZC3H7CHOO + HCHO = C4SOZC
1.70E-12	ZC3H7CHOO + C3H7CHO = C4SOZC4
$1.57E10*T^{1.03}*EXP(-7464/T)$	EC3H7CHOO = BUTACID
$1.58E-14*[H_2O]*0.73$	EC3H7CHOO = PRCHOHOOH
$1.58E-14*[H_2O]*0.06$	EC3H7CHOO = C3H7CHO + H2O2
$1.58E-14*[H_2O]*0.21$	EC3H7CHOO = BUTACID
$1.75E-11*[(H_2O)_2]*0.40$	EC3H7CHOO = PRCHOHOOH
$1.75E-11*[(H_2O)_2]*0.06$	EC3H7CHOO = C3H7CHO + H2O2
$1.75E-11*[(H_2O)_2]*0.54$	EC3H7CHOO = BUTACID
5.00E-10	EC3H7CHOO + HCOOH = HP1BUFORM
2.50E-10	EC3H7CHOO + BUTACID = HP1BUBUTR
1.70E-12	EC3H7CHOO + HCHO = C4SOZC
1.70E-12	EC3H7CHOO + C3H7CHO = C4SOZC4
OH initiation reactions	
$5.86E-12*EXP(500/T)*0.863$	PENT1ENE + OH = PE1ENEAO2
$5.86E-12*EXP(500/T)*0.137$	PENT1ENE + OH = PE1ENEBO2
RO₂ and RO chemistry	
KRO2HO2*0.498	NC3H7O2 + HO2 = NC3H7OOH
$1.00E-13*EXP(559/T)*0.2*[RO_2]$	NC3H7O2 = C2H5CHO
$1.00E-13*EXP(559/T)*0.6*[RO_2]$	NC3H7O2 = NC3H7O
$1.00E-13*EXP(559/T)*0.2*[RO_2]$	NC3H7O2 = NPROPOL
$2.6E-14*EXP(-255/T)*[O_2]$	NC3H7O = C2H5CHO + HO2
KRO2HO2*0.683*0.82	BUTALAO2 + HO2 = BUTALAOOH
KRO2HO2*0.683*0.18	BUTALAO2 + HO2 = BUTAL2O + OH
$1.00E-13*EXP(779/T)*0.6*[RO_2]$	BUTALAO2 = BUTAL2O
$1.00E-13*EXP(779/T)*0.2*[RO_2]$	BUTALAO2 = EGLYOX

1.00E-13*EXP(779/T)*0.2*[RO$_2$]	BUTALAO2 = HO3C3CHO
KDEC	BUTAL2O = C2H5CHO + HO2 + CO
KRO2HO2*0.748	PE1ENEAO2 + HO2 = C51OH2OOH
1.00E-13*EXP(731/T)*0.2*[RO$_2$]	PE1ENEAO2 = C51OH2CO
1.00E-13*EXP(731/T)*0.2*[RO$_2$]	PE1ENEAO2 = HO12C5
1.00E-13*EXP(731/T)*0.6*[RO$_2$]	PE1ENEAO2 = PE1ENEAO
1.80E+13*EXP(-4076/T)	PE1ENEAO = C3H7CHO + HCHO + HO2
KRO2HO2*0.748	PE1ENEBO2 + HO2 = C52OH1OOH
1.00E-13*EXP(1007/T)*0.2*[RO$_2$]	PE1ENEBO2 = C4OHCHO
1.00E-13*EXP(1007/T)*0.2*[RO$_2$]	PE1ENEBO2 = HO12C5
1.00E-13*EXP(1007/T)*0.6*[RO$_2$]	PE1ENEBO2 = PE1ENEBO
1.80E+13*EXP(-5234/T)	PE1ENEBO = C3H7CHO + HCHO + HO2
8.00E+10*EXP(-3010/T)	PE1ENEBO = HO12C54O2
KRO2HO2*0.800	HO12C54O2 + HO2 = HO12C54OOH
1.00E-13*EXP(373/T)*0.2*[RO$_2$]	HO12C54O2 = C51OH
1.00E-13*EXP(373/T)*0.2*[RO$_2$]	HO12C54O2 = HO124C5
1.00E-13*EXP(373/T)*0.6*[RO$_2$]	HO12C54O2 = HO12C54O
8.00E+10*EXP(-2417/T)	HO12C54O = HO24C4CHO + HO2
Hex-1-ene	
O$_3$ initiation reactions	
1.33E-15*EXP(-1480/T)*0.35	HEX1ENE + O3 = CH2OO + C4H9CHO
1.33E-15*EXP(-1480/T)*0.325	HEX1ENE + O3 = HCHO + ZC4H9CHOOA
1.33E-15*EXP(-1480/T)*0.325	HEX1ENE + O3 = HCHO + EC4H9CHOOA
Excited CI chemistry	
KDEC*0.25	ZC4H9CHOOA = ZC4H9CHOO
KDEC*0.75	ZC4H9CHOOA = C4CHOAO2 + OH
KDEC*0.25	EC4H9CHOOA = EC4H9CHOO
KDEC*0.288	EC4H9CHOOA = NC4H10
KDEC*0.166	EC4H9CHOOA = NBUTOL + CO
KDEC*0.107	EC4H9CHOOA = C3H7CHCO
KDEC*0.189	EC4H9CHOOA = NC4H9O2 + HO2
Stabilized sCI chemistry	
1.30E-10	CH2OO + PENTACID = HPMEPENT
1.70E-12	CH2OO + C4H9CHO = C5SOZC

$2.41E\text{-}62*T^{24.33}*EXP(2571/T)$	ZC4H9CHOO = C4CHOAO2 + OH
$1.51E\text{-}18*[H_2O]*0.73$	ZC4H9CHOO = BUCHOHOOH
$1.51E\text{-}18*[H_2O]*0.06$	ZC4H9CHOO = C4H9CHO + H2O2
$1.51E\text{-}18*[H_2O]*0.21$	ZC4H9CHOO = PENTACID
$4.31E\text{-}15*[(H_2O)_2]*0.40$	ZC4H9CHOO = BUCHOHOOH
$4.31E\text{-}15*[(H_2O)_2]*0.06$	ZC4H9CHOO = C4H9CHO + H2O2
$4.31E\text{-}15*[(H_2O)_2]*0.54$	ZC4H9CHOO = PENTACID
2.50E-10	ZC4H9CHOO + HCOOH = HP1PEFORM
1.70E-10	ZC4H9CHOO + PENTACID = HP1PEPENT
1.70E-12	ZC4H9CHOO + HCHO = C5SOZC
1.70E-12	ZC4H9CHOO + C4H9CHO = C5SOZC5
$1.57E10*T^{1.03}*EXP(-7464/T)$	EC4H9CHOO = PENTACID
$1.58E\text{-}14*[H_2O]*0.73$	EC4H9CHOO = BUCHOHOOH
$1.58E\text{-}14*[H_2O]*0.06$	EC4H9CHOO = C4H9CHO + H2O2
$1.58E\text{-}14*[H_2O]*0.21$	EC4H9CHOO = PENTACID
$1.75E\text{-}11*[(H_2O)_2]*0.40$	EC4H9CHOO = BUCHOHOOH
$1.75E\text{-}11*[(H_2O)_2]*0.06$	EC4H9CHOO = C4H9CHO + H2O2
$1.75E\text{-}11*[(H_2O)_2]*0.54$	EC4H9CHOO = PENTACID
5.00E-10	EC4H9CHOO + HCOOH = HP1PEFORM
2.50E-10	EC4H9CHOO + PENTACID = HP1PEPENT
1.70E-12	EC4H9CHOO + HCHO = C5SOZC
1.70E-12	EC4H9CHOO + C4H9CHO = C5SOZC5
OH initiation reactions	
3.70E-11*0.863	HEX1ENE + OH = C6OH5O2
3.70E-11*0.137	HEX1ENE + OH = HO5C6O2
RO₂ and RO chemistry	
KRO2HO2*0.601	NC4H9O2 + HO2 = NC4H9OOH
$1.00E\text{-}13*EXP(667/T)*0.2*[RO_2]$	NC4H9O2 = C3H7CHO
$1.00E\text{-}13*EXP(667/T)*0.2*[RO_2]$	NC4H9O2 = NBUTOL
$1.00E\text{-}13*EXP(667/T)*0.6*[RO_2]$	NC4H9O2 = NC4H9O
$8.9E\text{-}14*EXP(-550/T)*[O_2]$	NC4H9O = C3H7CHO + HO2
$4.6D10*EXP(-3570/T)$	NC4H9O = HO1C4O2
KRO2HO2*0.683	HO1C4O2 + HO2 = HO1C4OOH
$1.00E\text{-}13*EXP(746/T)*0.6*[RO_2]$	HO1C4O2 = HO1C4O
$1.00E\text{-}13*EXP(746/T)*0.2*[RO_2]$	HO1C4O2 = HOC3H6CHO
$1.00E\text{-}13*EXP(746/T)*0.2*[RO_2]$	HO1C4O2 = HOC4H8OH

8.74E+11*EXP(-3430/T)	HO1C4O = HOC3H6CHO + HO2
KRO2HO2*0.748*0.82	C4CHOAO2 + HO2 = C4CHOAOOH
KRO2HO2*0.748*0.18	C4CHOAO2 + HO2 = C4CHO2O + OH
1.00E-13*EXP(834/T)*0.6*[RO$_2$]	C4CHOAO2 = C4CHO2O
1.00E-13*EXP(834/T)*0.2*[RO$_2$]	C4CHOAO2 = C4OHCHO
1.00E-13*EXP(834/T)*0.2*[RO$_2$]	C4CHOAO2 = PGLYOX
KDEC	C4CHO2O = C3H7CHO + HO2 + CO
KRO2HO2*0.800	C6OH5O2 + HO2 = C6OH5OOH
1.00E-13*EXP(760/T)*0.2*[RO$_2$]	C6OH5O2 = C4COMEOH
1.00E-13*EXP(760/T)*0.2*[RO$_2$]	C6OH5O2 = C656OH
1.00E-13*EXP(760/T)*0.6*[RO$_2$]	C6OH5O2 = C6OH5O
1.80E+13*EXP(-4076/T)	C6OH5O = C4H9CHO + HCHO + HO2
8.00E+10*EXP(-3010/T)	C6OH5O = HO12C65O2
KRO2HO2*0.800	HO5C6O2 + HO2 = HO5C6OOH
1.00E-13*EXP(1021/T)*0.2*[RO$_2$]	HO5C6O2 = C656OH
1.00E-13*EXP(1021/T)*0.2*[RO$_2$]	HO5C6O2 = HO5C5CHO
1.00E-13*EXP(1021/T)*0.6*[RO$_2$]	HO5C6O2 = HO5C6O
1.80E+13*EXP(-5234/T)	HO5C6O = HCHO + C4H9CHO + HO2
8.00E+10*EXP(-3010/T)	HO5C6O = HO12C64O2
KRO2HO2*0.841	HO12C65O2 + HO2 = HO12C65OOH
1.00E-13*EXP(399/T)*0.2*[RO$_2$]	HO12C65O2 = HO12C65CO
1.00E-13*EXP(399/T)*0.2*[RO$_2$]	HO12C65O2 = HO125C6
1.00E-13*EXP(399/T)*0.6*[RO$_2$]	HO12C65O2 = HO12C65O
4.00E+10*EXP(-1871/T)	HO12C65O = HO15C62CO + HO2
KRO2HO2*0.841	HO12C64O2 + HO2 = HO12C64OOH
1.00E-13*EXP(399/T)*0.2*[RO$_2$]	HO12C64O2 = HO12C64CO
1.00E-13*EXP(399/T)*0.2*[RO$_2$]	HO12C64O2 = HO124C6
1.00E-13*EXP(399/T)*0.6*[RO$_2$]	HO12C64O2 = HO12C64O
8.00E+10*EXP(-2417/T)	HO12C64O = HO35C5CHO + HO2
cis-But-2-ene	
O$_3$ initiation reactions	
3.37E-15*EXP(-970/T)*0.33	CBUT2ENE + O3 = CH3CHO + ZCH3CHOOB
3.37E-15*EXP(-970/T)*0.67	CBUT2ENE + O3 = CH3CHO + ECH3CHOOB
Excited CI chemistry	
KDEC*0.50	ZCH3CHOOB = ZCH3CHOO

KDEC*0.50	ZCH3CHOOB = HCOCH2O2 + OH
KDEC*0.32	ECH3CHOOB = ECH3CHOO
KDEC*0.268	ECH3CHOOB = CH4
KDEC*0.138	ECH3CHOOB = CH3OH + CO
KDEC*0.104	ECH3CHOOB = CH2CO
KDEC*0.170	ECH3CHOOB = CH3O2 + HO2
OH initiation reactions	
1.10E-11*EXP(487/T)	CBUT2ENE + OH = BUT2OLO2
RO₂ and RO chemistry	
KRO2HO2*0.683	BUT2OLO2 + HO2 = BUT2OLOOH
1.00E-13*EXP(675/T)*0.6*[RO₂]	BUT2OLO2 = BUT2OLAO
1.00E-13*EXP(675/T)*0.2*[RO₂]	BUT2OLO2 = BUT2OLO
1.00E-13*EXP(675/T)*0.2*[RO₂]	BUT2OLO2 = BUT2OLOH
1.80E+13*EXP(-2528/T)	BUT2OLAO = CH3CHO + CH3CHO + HO2
trans-But-2-ene	
O₃ initiation reactions	
6.64E-15*EXP(-1059/T)*0.6	TBUT2ENE + O3 = CH3CHO + ZCH3CHOOB
6.64E-15*EXP(-1059/T)*0.4	TBUT2ENE + O3 = CH3CHO + ECH3CHOOC
Excited CI chemistry	
KDEC*0.32	ECH3CHOOC = ECH3CHOO
KDEC*0.288	ECH3CHOOC = CH4
KDEC*0.175	ECH3CHOOC = CH3OH + CO
KDEC*0.115	ECH3CHOOC = CH2CO
KDEC*0.102	ECH3CHOOC = CH3O2 + HO2
OH initiation reactions	
1.01E-11*EXP(550/T)	TBUT2ENE + OH = BUT2OLO2
trans-Pent-2-ene	
O₃ initiation reactions	
7.10E-15*EXP(-1132/T)*0.25	TPENT2ENE + O3 = ZC2H5CHOOB + CH3CHO
7.10E-15*EXP(-1132/T)*0.25	TPENT2ENE + O3 = EC2H5CHOOB + CH3CHO
7.10E-15*EXP(-1132/T)*0.25	TPENT2ENE + O3 = ZCH3CHOOC + C2H5CHO
7.10E-15*EXP(-1132/T)*0.25	TPENT2ENE + O3 = ECH3CHOOD + C2H5CHO
Excited CI chemistry	
KDEC*0.58	ZCH3CHOOC = ZCH3CHOO

KDEC*0.42	ZCH3CHOOC = HCOCH2O2 + OH
KDEC*0.58	ECH3CHOOD = ECH3CHOO
KDEC*0.178	ECH3CHOOD = CH4
KDEC*0.108	ECH3CHOOD = CH3OH + CO
KDEC*0.071	ECH3CHOOD = CH2CO
KDEC*0.063	ECH3CHOOD = CH3O2 + HO2
KDEC*0.45	ZC2H5CHOOB = ZC2H5CHOO
KDEC*0.55	ZC2H5CHOOB = PROPALO2 + OH
KDEC*0.45	EC2H5CHOOB = EC2H5CHOO
KDEC*0.233	EC2H5CHOOB = C2H6
KDEC*0.141	EC2H5CHOOB = C2H5OH + CO
KDEC*0.093	EC2H5CHOOB = CH3CHCO
KDEC*0.083	EC2H5CHOOB = C2H5O2 + HO2
Stabilized sCI chemistry	
1.70E-10	ZCH3CHOO + PROPACID = HP1ETPROP
1.70E-12	ZCH3CHOO + C2H5CHO = C3SOZC2
2.50E-10	ECH3CHOO + PROPACID = HP1ETPROP
1.70E-12	ECH3CHOO + C2H5CHO = C3SOZC2
1.70E-10	ZC2H5CHOO + CH3CO2H = HP1PRACET
1.70E-12	ZC2H5CHOO + CH3CHO = C3SOZC2
2.50E-10	EC2H5CHOO + CH3CO2H = HP1PRACET
1.70E-12	EC2H5CHOO + CH3CHO = C3SOZC2
OH initiation reactions	
6.69E-11*0.5	TPENT2ENE + OH = PE2ENEAO2
6.69E-11*0.5	TPENT2ENE + OH = PE2ENEBO2
RO$_2$ and RO chemistry	
KRO2HO2*0.748	PE2ENEAO2 + HO2 = C52OH3OOH
1.00E-13*EXP(731/T)*0.2*[RO$_2$]	PE2ENEAO2 = C523OH
1.00E-13*EXP(731/T)*0.2*[RO$_2$]	PE2ENEAO2 = DIEKAOH
1.00E-13*EXP(731/T)*0.6*[RO$_2$]	PE2ENEAO2 = PE2ENEAO
1.80E+13*EXP(-2528/T)	PE2ENEAO = C2H5CHO + CH3CHO + HO2

KRO2HO2*0.748	PE2ENEBO2 + HO2 = C53OH2OOH
1.00E-13*EXP(731/T)*0.2*[RO$_2$]	PE2ENEBO2 = C523OH
1.00E-13*EXP(731/T)*0.2*[RO$_2$]	PE2ENEBO2 = MPRKAOH
1.00E-13*EXP(731/T)*0.6*[RO$_2$]	PE2ENEBO2 = PE2ENEBO
1.80E+13*EXP(-2528/T)	PE2ENEBO = CH3CHO + C2H5CHO + HO2
trans-Hex-2-ene	
O$_3$ initiation reactions	
7.60E-15*EXP(-1163/T)*0.25	THEX2ENE + O3 = C3H7CHO + ZCH3CHOOD
7.60E-15*EXP(-1163/T)*0.25	THEX2ENE + O3 = C3H7CHO + ECH3CHOOE
7.60E-15*EXP(-1163/T)*0.25	THEX2ENE + O3 = CH3CHO + ZC3H7CHOOB
7.60E-15*EXP(-1163/T)*0.25	THEX2ENE + O3 = CH3CHO + EC3H7CHOOB
Excited CI chemistry	
KDEC*0.80	ZCH3CHOOD = ZCH3CHOO
KDEC*0.20	ZCH3CHOOD = HCOCH2O2 + OH
KDEC*0.80	ECH3CHOOE = ECH3CHOO
KDEC*0.085	ECH3CHOOE = CH4
KDEC*0.051	ECH3CHOOE = CH3OH + CO
KDEC*0.034	ECH3CHOOE = CH2CO
KDEC*0.030	ECH3CHOOE = CH3O2 + HO2
KDEC*0.40	ZC3H7CHOOB = ZC3H7CHOO
KDEC*0.60	ZC3H7CHOOB = BUTALAO2 + OH
KDEC*0.40	EC3H7CHOOB = ECH3CHOO
KDEC*0.254	EC3H7CHOOB = C3H8
KDEC*0.155	EC3H7CHOOB = NPROPOL + CO
KDEC*0.101	EC3H7CHOOB = C2H5CHCO
KDEC*0.090	EC3H7CHOOB = NC3H7O2 + HO2
Stabilized sCI chemistry	
1.70E-10	ZCH3CHOO + BUTACID = HP1ETBUTR
1.70E-12	ZCH3CHOO + C3H7CHO = C4SOZC2
2.50E-10	ECH3CHOO + BUTACID = HP1ETBUTR
1.70E-12	ECH3CHOO + C3H7CHO = C4SOZC2
1.70E-10	ZC3H7CHOO + CH3CO2H = HP1BUACET
1.70E-12	ZC3H7CHOO + CH3CHO = C4SOZC2

2.50E-10	EC3H7CHOO + CH3CO2H = HP1BUACET
1.70E-12	EC3H7CHOO + CH3CHO = C4SOZC2
OH initiation reactions	
6.00E-11*0.5	THEX2ENE + OH = C64OH5O2
6.00E-11*0.5	THEX2ENE + OH = C65OH4O2
RO₂ and RO chemistry	
KRO2HO2*0.800	C64OH5O2 + HO2 = C64OH5OOH
1.00E-13*EXP(760/T)*0.2*[RO₂]	C64OH5O2 = C645OH
1.00E-13*EXP(760/T)*0.6*[RO₂]	C64OH5O2 = C64OH5O
1.00E-13*EXP(760/T)*0.2*[RO₂]	C64OH5O2 = CO2HO3C6
1.80E+13*EXP(-2528/T)	C64OH5O = CH3CHO + C3H7CHO + HO2
KRO2HO2*0.800	C65OH4O2 + HO2 = C65OH4OOH
1.00E-13*EXP(760/T)*0.2*[RO₂]	C65OH4O2 = C645OH
1.00E-13*EXP(760/T)*0.6*[RO₂]	C65OH4O2 = C65OH4O
1.00E-13*EXP(760/T)*0.2*[RO₂]	C65OH4O2 = HEX3ONCOH
1.80E+13*EXP(-2528/T)	C65OH4O = C3H7CHO + CH3CHO + HO2
2-Methyl-but-2-ene	
O₃ initiation reactions	
6.51E-15*EXP(-829/T)*0.63	ME2BUT2ENE + O3= CH3CHO + CH3CCH3OOA
6.51E-15*EXP(-829/T)*0.22	ME2BUT2ENE + O3= CH3COCH3 + ZCH3CHOOE
6.51E-15*EXP(-829/T)*0.15	ME2BUT2ENE + O3= CH3COCH3 + ECH3CHOOF
Excited CI chemistry	
KDEC*0.35	ZCH3CHOOE = ZCH3CHOO
KDEC*0.65	ZCH3CHOOE = HCOCH2O2 + OH
KDEC*0.35	ECH3CHOOF = ECH3CHOO
KDEC*0.275	ECH3CHOOF = CH4
KDEC*0.167	ECH3CHOOF = CH3OH + CO
KDEC*0.110	ECH3CHOOF = CH2CO
KDEC*0.098	ECH3CHOOF = CH3O2 + HO2
KDEC*0.27	CH3CCH3OOA = CH3CCH3OO
KDEC*0.73	CH3CCH3OOA = CH3COCH2O2 + OH
Stabilized sCI chemistry	
7.2E+06*EXP(-2920/T)	CH3CCH3OO = CH3COCH2O2 + OH

7.54E-18*H2O*0.92	CH3CCH3OO = H2IPROOH
7.54E-18*H2O*0.08	CH3CCH3OO = CH3COCH3 + H2O2
1.82E-14*H2OD*0.87	CH3CCH3OO = H2IPROOH
1.82E-14*H2OD*0.13	CH3CCH3OO = CH3COCH3 + H2O2
3.10E-10	CH3CCH3OO + CH3CO2H = HP2PRACET
1.70E-12	CH3CCH3OO + CH3CHO = IC3SOZC2
3.40E-13	CH3CCH3OO + CH3COCH3 = IC3SOZIC3
3.40E-13	ZCH3CHOO + CH3COCH3 = IC3SOZC2
3.40E-13	ECH3CHOO + CH3COCH3 = IC3SOZC2
OH initiation reactions	
1.92E-11*EXP(450/T)*0.353	ME2BUT2ENE + OH = ME2BU2OLO2
1.92E-11*EXP(450/T)*0.647	ME2BUT2ENE + OH = ME2BUOLO2
RO$_2$ and RO chemistry	
1.15E-13*EXP(1300/T)*0.18	CH3COCH2O2 + HO2 = CH3COCH2O + OH
1.15E-13*EXP(1300/T)*0.82	CH3COCH2O2 + HO2 = HYPERACET
1.00E-13*EXP(1045/T)*0.2*[RO$_2$]	CH3COCH2O2 = ACETOL
1.00E-13*EXP(1045/T)*0.6*[RO$_2$]	CH3COCH2O2 = CH3COCH2O
1.00E-13*EXP(1045/T)*0.2*[RO$_2$]	CH3COCH2O2 = MGLYOX
KDEC	CH3COCH2O = CH3CO3 + HCHO
4.40E-15*EXP(1910/T)	CH3CO3 + HO2 = CH3CO2H + O3
1.50E-12*EXP(480/T)	CH3CO3 + HO2 = CH3CO3H
4.66E-12*EXP(235/T)	CH3CO3 + HO2 = CH3O2 + OH
2.00E-12*EXP(508/T)*0.2*[RO$_2$]	CH3CO3 = CH3CO2H
2.00E-12*EXP(508/T)*0.8*[RO$_2$]	CH3CO3 = CH3O2
KRO2HO2*0.748	ME2BU2OLO2 + HO2 = M2BU2OLOOH
1.00E-13*EXP(731/T)*0.2*[RO$_2$]	ME2BU2OLO2 = C4ME3HO23
1.00E-13*EXP(731/T)*0.6*[RO$_2$]	ME2BU2OLO2 = ME2BU2OLO
1.00E-13*EXP(731/T)*0.2*[RO$_2$]	ME2BU2OLO2 = MIPKAOH
1.80E+13*EXP(-1424/T)	ME2BU2OLO = CH3COCH3 + CH3CHO + HO2
KRO2HO2*0.748	ME2BUOLO2 + HO2 = ME2BUOLOOH
1.00E-13*EXP(221/T)*0.2*[RO$_2$]	ME2BUOLO2 = C4ME3HO23
1.00E-13*EXP(221/T)*0.8*[RO$_2$]	ME2BUOLO2 = ME2BUOLO
1.80E+13*EXP(-1734/T)	ME2BUOLO = CH3COCH3 + CH3CHO + HO2
2,4,4-Trimethyl-pent-2-ene	
O$_3$ initiation reactions	

1.42E-16*0.8	TMEPEN2ENE + O3 = TBUTCHO + CH3CCH3OOB
1.42E-16*0.1	TMEPEN2ENE + O3 = CH3COCH3 + ZTBUCHOOA
1.42E-16*0.1	TMEPEN2ENE + O3 = CH3COCH3 + ETBUCHOOA
Excited CI chemistry	
KDEC*0.6	ZTBUCHOOA = ZTBUCHOO
KDEC*0.212	ZTBUCHOOA = IC4H10
KDEC*0.084	ZTBUCHOOA = TBUTOL + CO
KDEC*0.104	ZTBUCHOOA = TC4H9O2 + HO2
KDEC*0.6	ETBUCHOOA = ZTBUCHOO
KDEC*0.212	ETBUCHOOA = IC4H10
KDEC*0.084	ETBUCHOOA = TBUTOL + CO
KDEC*0.104	ETBUCHOOA = TC4H9O2 + HO2
KDEC*0.6	CH3CCH3OOB = CH3CCH3OO
KDEC*0.4	CH3CCH3OOB = CH3COCH2O2 + OH
Stabilized sCI chemistry	
2.58E6*T$^{2.32}$*EXP(-9710/T)	ZTBUCHOO = TBUTCO2H
2.40E-19*H2O*0.73	ZTBUCHOO = TBUCHOHOOH
2.40E-19*H2O*0.06	ZTBUCHOO = TBUTCHO + H2O2
2.40E-19*H2O*0.21	ZTBUCHOO = TBUTCO2H
2.84E-15*H2OD*0.40	ZTBUCHOO = TBUCHOHOOH
2.84E-15*H2OD*0.06	ZTBUCHOO = TBUTCHO + H2O2
2.84E-15*H2OD*0.54	ZTBUCHOO = TBUTCO2H
1.70E-10	ZTBUCHOO + CH3CO2H = HPNPACET
1.70E-12	ZTBUCHOO + CH3CHO = NPC5SOZC2
1.70E-10	ZTBUCHOO + TBUTCO2H = HPNPPIV
1.70E-12	ZTBUCHOO + TBUTCHO = NPSOZNP
3.40E-13	ZTBUCHOO + CH3COCH3 = NPSOZIC3
8.51E9*T$^{1.15}$*EXP(-7357/T)	ETBUCHOO = TBUTCO2H
4.50E-14*H2O*0.73	ETBUCHOO = TBUCHOHOOH
4.50E-14*H2O*0.06	ETBUCHOO = TBUTCHO + H2O2
4.50E-14*H2O*0.21	ETBUCHOO = TBUTCO2H
4.74E-11*H2OD*0.40	ETBUCHOO = TBUCHOHOOH
4.74E-11*H2OD*0.06	ETBUCHOO = TBUTCHO + H2O2
4.74E-11*H2OD*0.54	ETBUCHOO = TBUTCO2H

2.50E-10	ETBUCHOO + CH3CO2H = HPNPACET
1.70E-12	ETBUCHOO + CH3CHO = NPC5SOZC2
2.50E-10	ETBUCHOO + TBUTCO2H = HPNPPIV
1.70E-12	ETBUCHOO + TBUTCHO = NPSOZNP
3.40E-13	ETBUCHOO + CH3COCH3 = NPSOZIC3
3.10E-10	CH3CCH3OO + TBUTCO2H = HP2PRPIV
1.70E-12	CH3CCH3OO + TBUTCHO = NPSOZIC3
OH initiation reactions	
8.0E-11*0.338	TMEPEN2ENE + OH = HOC8AO2
8.0E-11*0.662	TMEPEN2ENE + OH = HOC8BO2
RO$_2$ and RO chemistry	
KRO2HO2*0.601	TC4H9O2 + HO2 = TC4H9OOH
1.00E-13*EXP(-662/T)*0.2*[RO$_2$]	TC4H9O2 = TBUTOL
1.00E-13*EXP(-662/T)*0.8*[RO$_2$]	TC4H9O2 = TC4H9O
6.00E+14*EXP(-8153/T)	TC4H9O = CH3COCH3 + CH3O2
KRO2HO2*0.874	HOC8AO2 + HO2 = HOC8AOOH
1.00E-13*EXP(783/T)*0.2*[RO$_2$]	HOC8AO2 = HOC8ACO
1.00E-13*EXP(783/T)*0.6*[RO$_2$]	HOC8AO2 = HOC8AO
1.00E-13*EXP(783/T)*0.2*[RO$_2$]	HOC8AO2 = HOC8AOH
1.80E+13*EXP(-4076/T)	HOC8AO = CH3COCH3 + TBUTCHO + HO2
KRO2HO2*0.874	HOC8BO2 + HO2 = HOC8BOOH
1.00E-13*EXP(221/T)*0.2*[RO$_2$]	HOC8BO2 = HOC8AOH
1.00E-13*EXP(221/T)*0.8*[RO$_2$]	HOC8BO2 = HOC8BO
1.80E+13*EXP(-1734/T)	HOC8BO = CH3COCH3 + TBUTCHO + HO2
Cyclohexene	
O$_3$ initiation reactions	
2.80E-15*EXP(-1063/T)*0.62	CHEXENE + O3 = ZC6COCHOOA
2.80E-15*EXP(-1063/T)*0.38	CHEXENE + O3 = EC6COCHOOA
Excited CI chemistry	
KDEC*0.030	ZC6COCHOOA = ZC6COCHOO
KDEC*0.970	ZC6COCHOOA = ADIP2O2 + OH
KDEC*0.030	EC6COCHOOA = EC6COCHOO
KDEC*0.314	EC6COCHOOA = ADIPAL + O
KDEC*0.621	EC6COCHOOA = C4H9CHO

KDEC*0.035	EC6COCHOOA = HCOC4CO2H
Stabilized sCI chemistry	
KDEC	ZC6COCHOO = CHEXSOZ
KDEC	EC6COCHOO = CHEXSOZ
OH initiation reaction	
6.77E-11	CHEXENE + OH = HOCHEXO2
RO$_2$ and RO chemistry	
KRO2HO2*0.800	HOCHEXO2 + HO2 = HOCHEXOOH
1.00E-13*EXP(760/T)*0.2*[RO$_2$]	HOCHEXO2 = HOCHEXCO
1.00E-13*EXP(760/T)*0.6*[RO$_2$]	HOCHEXO2 = HOCHEXO
1.00E-13*EXP(760/T)*0.2*[RO$_2$]	HOCHEXO2 = HOCHEXOH
KDEC	HOCHEXO = ADIPAL + HO2
2.91E-30*T$^{12.9}$*EXP(-2167/T)	ADIP2O2 = CO6HP5CO3
1.08E-66*T$^{25.23}$*EXP(1616/T)	ADIP2O2 = GLUTAL + CO + OH
5.64E-20*T$^{8.46}$*EXP(945/T)	CO6HP5CO3 = C6HOM1O2
5.64E-20*T$^{8.46}$*EXP(-586/T)	C6HOM1O2 = CO6HP5CO3
2.01E-52*T$^{19.91}$*EXP(1765/T)	CO6HP5CO3 = CO65CO3H + OH
1.08E-66*T$^{25.23}$*EXP(1616/T)	C6HOM1O2 = HCOC3CO3H + CO + OH
KRO2HO2*0.841*0.82	ADIP2O2 + HO2 = ADIP2OOH
KRO2HO2*0.841*0.18	ADIP2O2 + HO2 = ADIP2O + OH
1.00E-13*EXP(878/T)*0.2*[RO$_2$]	ADIP2O2 = ADIP2CO
1.00E-13*EXP(878/T)*0.6*[RO$_2$]	ADIP2O2 = ADIP2O
1.00E-13*EXP(878/T)*0.2*[RO$_2$]	ADIP2O2 = ADIP2OH
KDEC	ADIP2O = GLUTAL + CO + HO2
3.00E-12*EXP(480/T)*0.900	CO6HP5CO3 + HO2 = CO6HP5CO3H
8.83E-15*EXP(1910/T)*0.900	CO6HP5CO3 + HO2 = CO6HP5CO2H + O3
9.35E-12*EXP(235/T)*0.900	CO6HP5CO3 + HO2 = CO5HP4O2 + OH
2.00E-12*EXP(508/T)*0.2*[RO$_2$]	CO6HP5CO3 = CO6HP5CO2H
2.00E-12*EXP(508/T)*0.8*[RO$_2$]	CO6HP5CO3 = CO5HP4O2
KRO2HO2*0.900*0.82	C6HOM1O2 + HO2 = CO6HP5CO3H
KRO2HO2*0.900*0.18	C6HOM1O2 + HO2 = C6HOM1O + OH
1.00E-13*EXP(891/T)*0.2*[RO$_2$]	C6HOM1O2 = CO65CO3H
1.00E-13*EXP(891/T)*0.6*[RO$_2$]	C6HOM1O2 = C6HOM1O
1.00E-13*EXP(891/T)*0.2*[RO$_2$]	C6HOM1O2 = C6HOM1OH

KDEC	C6HOM1O = HCOC3CO3H + CO + HO2
$3.48E{-}25*T^{10.16}*EXP(1327/T)$	CO5HP4O2 = CO1HP5O2
$9.14E{-}15*T^{6.76}*EXP({-}423/T)$	CO1HP5O2 = CO5HP4O2
$2.91E{-}30*T^{12.9}*EXP({-}1458/T)$	CO5HP4O2 = HP4CHO + CO + OH
$1.07E{-}64*T^{23.93}*EXP(3106/T)$	CO5HP4O2 = HP5GLYOX + OH
$1.08E{-}66*T^{25.23}*EXP(1616/T)$	CO1HP5O2 = HP4CHO + CO + OH
KRO2HO2*0.841	CO5HP4O2 + HO2 = CO5HP4OOH
1.00E-13*EXP(821/T)*0.2*[RO2]	CO5HP4O2 = CO5HP4CHO
1.00E-13*EXP(821/T)*0.6*[RO2]	CO5HP4O2 = CO5HP4O
1.00E-13*EXP(821/T)*0.2*[RO2]	CO5HP4O2 = CO5HP4OH
KDEC	CO5HP4O = HOC3H6CHO + CO + OH
KRO2HO2*0.841*0.82	CO1HP5O2 + HO2 = CO5HP4OOH
KRO2HO2*0.841*0.18	CO1HP5O2 + HO2 = CO1HP5O + OH
1.00E-13*EXP(878/T)*0.2*[RO2]	CO1HP5O2 = HP5GLYOX
1.00E-13*EXP(878/T)*0.6*[RO2]	CO1HP5O2 = CO1HP5O
1.00E-13*EXP(878/T)*0.2*[RO2]	CO1HP5O2 = CO1HP5OH
KDEC	CO1HP5O = HP4CHO + CO + HO2
Inorganic reactions	
$6.0E{-}34*[M]*(T/300)^{-2.6}*[O_2]$	O = O3
8.0E-12*EXP(-2060/T)	O + O3 =
1.70E-12*EXP(-940/T)	OH + O3 = HO2
$2.03E{-}16*(T/300)^{4.57}*EXP(693/T)$	HO2 + O3 = OH
2.20E-13*EXP(600/T)*F_{H2O} [g]	HO2 + HO2 = H2O2
1.90E-33*[M]*EXP(980/T)*F_{H2O}	HO2 + HO2 = H2O2

Comments

[a] Reaction mechanism is designed for application to single alkene systems, but complete listing must be used for common chemistry to be represented;

[b] Units are cm^3 molecule^{-1} s^{-1} for bimolecular reactions or s^{-1} for unimolecular (or pseudo-unimolecular) reactions;

[c] KDEC is a generic parameter applied to selected very rapid reactions for convenience, and was assigned a value of 1.0E+06 s^{-1} in these calculations;

[d] KMT16 is the rate coefficient for a pressure-dependent reaction in the fall-off regime, with k_0 = 8.0E-27*[M]*(T/300)$^{-3.5}$ cm^3 molecule^{-1} s^{-1}, k_∞ = 3.0E-11*(T/300)$^{-1}$ cm^3 molecule^{-1} s^{-1}, and F_c = 0.5;

[e] KRO2HO2 = 2.80E-13*EXP(1300/T);

[f] [RO2] represents the concentration sum of all peroxy radicals in the system;

[g] F_{H2O} = 1 + (1.40E-21*EXP(2200/T)*[H2O]).

Table S5: Identities of the organic species in the updated chemical schemes listed in Table S4 [a].

Species	SMILES [b]	Species	SMILES
C3H6	CC=C	C656OH	CCCCC(O)CO
CH2OOA	C=[O+][O-] [c]	C6OH5O	CCCCC([O])CO
CH2OO	C=[O+][O-]	HO5C6O2	CCCCC(O)CO[O]
ZCH3CHOOA	[O-]\[O+]=C/C [c]	HO5C6OOH	CCCCC(O)COO
ZCH3CHOO	[O-]\[O+]=C/C	HO5C5CHO	CCCCC(O)C=O
ECH3CHOOA	[O-]/[O+]=C/C [c]	HO5C6O	CCCCC(O)C[O]
ECH3CHOO	[O-]/[O+]=C/C	HO12C65O2	CC(O[O])CCC(O)CO
HCHO	C=O	HO12C65OOH	CC(OO)CCC(O)CO
CH3CHO	CC=O	HO12C65CO	CC(CCC(O)CO)=O
CH4	C	HO125C6	CC(O)CCC(O)CO
CH3OH	CO	HO12C65O	CC([O])CCC(O)CO
CH2CO	C=C=O	HO15C62CO	CC(O)CCC(CO)=O
HOCH2OOH	OCOO	HO12C64O2	CCC(O[O])CC(O)CO
HCOOH	O=CO	HO12C64OOH	CCC(OO)CC(O)CO
HPMEFORM	O=COCOO	HO12C64CO	CCC(CC(O)CO)=O
HPMEACET	O=C(C)OCOO	HO124C6	CCC(O)CC(O)CO
CSOZC	C1OOCO1	HO12C64O	CCC([O])CC(O)CO
C2SOZC	CC1OOCO1	HO35C5CHO	CCC(O)CC(O)C=O
CH3CHOHOOH	CC(OO)O	CBUT2ENE	C\C=C/C
CH3CO2H	O=C(O)C	ZCH3CHOOB	[O-]\[O+]=C/C [c]
HP1ETFORM	O=COC(C)OO	ECH3CHOOB	[O-]/[O+]=C/C [c]
HP1ETACET	O=C(C)OC(C)OO	BUT2OLO2	[O]OC(C)C(C)O
C2SOZC2	CC1OOC(C)O1	BUT2OLOOH	OOC(C)C(C)O
HCOCH2O2	O=CCO[O]	BUT2OLO	CC(=O)C(C)O
HCOCH2OOH	O=CCOO	BUT2OLOH	CC(O)C(C)O
GLYOX	O=CC=O	BUT2OLAO	CC([O])C(C)O
HOCH2CHO	OCC=O	TBUT2ENE	C/C=C/C
HCOCH2O	[O]CC=O	ECH3CHOOC	[O-]/[O+]=C/C [c]
CH3O2	CO[O]	TPENT2ENE	CC/C=C/C
CH3OOH	COO	ZC2H5CHOOB	[O-]\[O+]=C/CC [c]
CH3O	C[O]	EC2H5CHOOB	[O-]/[O+]=C/CC [c]
HYPROPO2	CC(CO)O[O]	ZCH3CHOOC	[O-]\[O+]=C/C [c]
HYPROPO2H	CC(CO)OO	ECH3CHOOD	[O-]/[O+]=C/C [c]

ACETOL	CC(CO)=O	HP1ETPROP	CCC(OC(C)OO)=O
PROPGLY	CC(CO)O	C3SOZC2	CC1OOC(CC)O1
HYPROPO	CC(CO)[O]	HP1PRACET	CC(OC(CC)OO)=O
IPROPOLO2	CC(CO[O])O	PE2ENEAO2	CCC(O[O])C(O)C
IPROPOLO2H	CC(COO)O	C52OH3OOH	CCC(OO)C(O)C
CH3CHOHCHO	CC(C=O)O	C523OH	CCC(O)C(O)C
IPROPOLO	CC(C[O])O	DIEKAOH	CCC(C(O)C)=O
BUT1ENE	CCC=C	PE2ENEAO	CCC([O])C(O)C
CH2OOB	C=[O+][O-] [c]	PE2ENEBO2	CCC(O)C(O[O])C
ZC2H5CHOOA	[O-]\[O+]=C/CC [c]	C53OH2OOH	CCC(O)C(OO)C
ZC2H5CHOO	[O-]\[O+]=C/CC	MPRKAOH	CCC(O)C(C)=O
EC2H5CHOOA	[O-]/[O+]=C/CC [c]	PE2ENEBO	CCC(O)C([O])C
EC2H5CHOO	[O-]/[O+]=C/CC	THEX2ENE	C/C=C/CCC
C2H6	CC	ZCH3CHOOD	[O-]\[O+]=C/C [c]
C2H5OH	CCO	ECH3CHOOE	[O-]/[O+]=C/C [c]
CH3CHCO	CC=C=O	ZC3H7CHOOB	CCC\C=[O+]/[O-] [c]
PROPACID	CCC(O)=O	EC3H7CHOOB	CCC/C=[O+]/[O-] [c]
C2H5CHO	CCC=O	HP1ETBUTR	O=C(OC(C)OO)CCC
HPMEPROP	O=C(CC)OCOO	C4SOZC2	CC1OOC(CCC)O1
C3SOZC	CCC1OOCO1	HP1BUACET	CC(OC(CCC)OO)=O
ETCHOHOOH	OC(OO)CC	C64OH5O2	CC(O[O])C(O)CCC
HP1PRFORM	O=COC(CC)OO	C64OH5OOH	CC(OO)C(O)CCC
HP1PRPROP	O=C(CC)OC(CC)OO	C645OH	CC(O)C(O)CCC
C3SOZC3	CCC1OOC(CC)O1	CO2HO3C6	CC(C(O)CCC)=O
C2H5O2	CCO[O]	C64OH5O	CC([O])C(O)CCC
C2H5OOH	CCOO	C65OH4O2	CC(O)C(O[O])CCC
C2H5O	CC[O]	C65OH4OOH	CC(O)C(OO)CCC
PROPALO2	CC(O[O])C=O	HEX3ONCOH	CC(O)C(CCC)=O
PROPALOOH	CC(OO)C=O	C65OH4O	CC(O)C([O])CCC
CH3CHOHCHO	CC(O)C=O	ME2BUT2ENE	CC(C)=CC
MGLYOX	CC(C=O)=O	CH3CCH3OOA	CC(C)=[O+][O-] [c]
PROPALO	CC([O])C=O	CH3CCH3OO	CC(C)=[O+][O-]
HO3C4O2	OC(CO[O])CC	ZCH3CHOOE	[O-]\[O+]=C/C [c]
HO3C4OOH	OC(COO)CC	ECH3CHOOF	[O-]\[O+]=C/C [c]
HO3C3CHO	OC(C=O)CC	CH3COCH3	CC(C)=O
NBUTOLAOH	OC(CO)CC	H2IPROOH	CC(C)(OO)O

HO3C4O	OC(C[O])CC	HP2PRACET	CC(C)(OO)OC(C)=O
NBUTOLAO2	CCC(O[O])CO	IC3SOZC2	CC1OOC(C)(C)O1
NBUTOLAOOH	CCC(OO)CO	IC3SOZIC3	CC1(C)OOC(C)(C)O1
MEKCOH	O=C(CO)CC	CH3COCH2O2	CC(CO[O])=O
NBUTOLAO	[O]C(CO)CC	HYPERACET	CC(COO)=O
HO34C4O2	OCC(O)CCO[O]	CH3COCH2O	CC(C[O])=O
HO34C4OOH	OCC(O)CCOO	CH3CO3	CC(O[O])=O
HO34C3CHO	OCC(O)CC=O	CH3CO3H	CC(OO)=O
HO13C4OH	OCC(O)CCO	ME2BU2OLO2	CC(C)(O)C(O[O])C
HO13C3CHO	O=CC(O)CCO	M2BU2OLOOH	CC(C)(O)C(OO)C
HO34C4O	OCC(O)CC[O]	C4ME3HO23	CC(C)(O)C(O)C
PENT1ENE	CCCC=C	MIPKAOH	CC(C)(O)C(C)=O
CH2OOC	C=[O+][O-] c	ME2BU2OLO	CC(C)(O)C([O])C
ZC3H7CHOOA	CCC\C=[O+]/[O-] c	ME2BUOLO2	CC(C)(O[O])C(O)C
ZC3H7CHOO	CCC\C=[O+]/[O-]	ME2BUOLOOH	CC(C)(OO)C(O)C
EC3H7CHOOA	CCC/C=[O+]/[O-] c	ME2BUOLO	CC(C)([O])C(O)C
EC3H7CHOO	CCC/C=[O+]/[O-]	TMEPEN2ENE	CC(C)=CC(C)(C)C
C3H7CHO	CCCC=O	CH3CCH3OOB	CC(C)=[O+][O-] c
C3H8	CCC	ZTBUCHOOA	CC(C)(C)/C=[O+]/[O-] c
NPROPOL	CCCO	ZTBUCHOO	CC(C)(C)/C=[O+]/[O-]
C2H5CHCO	CCC=C=O~~CCC1=[O]1~~	ETBUCHOOA	CC(C)(C)/C=[O+]\[O-] c
BUTACID	CCCC(O)=O	ETBUCHOO	CC(C)(C)/C=[O+]\[O-]
HPMEBUTR	CCCC(OCOO)=O	IC4H10	CC(C)C
C4SOZC	CCCC1OOCO1	TBUTOL	CC(C)(O)C
PRCHOHOOH	CCCC(OO)O	TBUTCO2H	CC(C)(C(O)=O)C
HP1BUFORM	O=COC(CCC)OO	TBUCHOHOOH	CC(C)(C(O)OO)C
HP1BUBUTR	CCCC(OC(CCC)OO)=O	TBUTCHO	CC(C)(C=O)C
C4SOZC4	CCCC1OOC(CCC)O1	HPNPACET	CC(C)(C(OC(C)=O)OO)C
NC3H7O2	CCCO[O]	NPC5SOZC2	CC1OOC(C(C)(C)C)O1
NC3H7OOH	CCCOO	HPNPPIV	CC(C)(C(OC(C(C)(C)C)=O)OO)C
NC3H7O	CCC[O]	NPSOZNP	CC(C)(C)C1OOC(C(C)(C)C)O1
BUTALAO2	CCC(C=O)O[O]	NPSOZIC3	CC1(C)OOC(C(C)(C)C)O1
BUTALAOOH	CCC(C=O)OO	HP2PRPIV	CC(OC(C(C)(C)C)=O)(C)OO
EGLYOX	CCC(C=O)=O	TC4H9O2	CC(C)(O[O])C
BUTAL2O	CCC(C=O)[O]	TC4H9OOH	CC(C)(OO)C
PE1ENEAO2	CCCC(O[O])CO	TC4H9O	CC(C)([O])C

42

C51OH2OOH	CCCC(CO)OO	HOC8AO2	CC(C)(O)C(O[O])C(C)(C)C
C51OH2CO	CCCC(=O)CO	HOC8AOOH	CC(C)(O)C(OO)C(C)(C)C
HO12C5	CCCC(O)CO	HOC8ACO	CC(C)(O)C(C(C)(C)C)=O
PE1ENEAO	CCCC([O])CO	HOC8AOH	CC(C)(O)C(O)C(C)(C)C
PE1ENEBO2	CCCC(O)CO[O]	HOC8AO	CC(C)(O)C([O])C(C)(C)C
C52OH1OOH	CCCC(O)COO	HOC8BO2	CC(C)(O[O])C(O)C(C)(C)C
C4OHCHO	CCCC(O)C=O	HOC8BOOH	CC(C)(OO)C(O)C(C)(C)C
PE1ENEBO	CCCC(O)C[O]	HOC8BO	CC(C)([O])C(O)C(C)(C)C
HO12C54O2	OCC(O)CC(C)O[O]	CHEXENE	C1CCCC=C1
HO12C54OOH	OCC(O)CC(C)OO	ZC6COCHOOA	O=CCCCC/C=[O+]\[O-] [c]
C51OH	OCC(O)CC(C)=O	ZC6COCHOO	O=CCCCC/C=[O+]\[O-]
HO124C5	OCC(O)CC(C)O	EC6COCHOOA	O=CCCCC/C=[O+]/[O-] [c]
HO24C4CHO	O=CC(O)CC(C)O	EC6COCHOO	O=CCCCC/C=[O+]/[O-]
HO12C54O	OCC(O)CC(C)[O]	HCOC4CO2H	O=CCCCCC(O)=O
HEX1ENE	CCCCC=C	CHEXSOZ	C12CCCCC(OO2)O1
ZC4H9CHOOA	CCCC\C=[O+]/[O-] [c]	HOCHEXO2	OC1C(O[O])CCCC1
ZC4H9CHOO	CCCC\C=[O+]/[O-]	HOCHEXOOH	OC1C(OO)CCCC1
EC4H9CHOOA	CCCC/C=[O+]/[O-] [c]	HOCHEXCO	OC1C(CCCC1)=O
EC4H9CHOO	CCCC/C=[O+]/[O-]	HOCHEXOH	OC1C(O)CCCC1
C4H9CHO	CCCCC=O	HOCHEXO	OC1C([O])CCCC1
NC4H10	CCCC	ADIPAL	O=CCCCCC=O
NBUTOL	CCCCO	ADIP2O2	O=CCCCC(O[O])C=O
C3H7CHCO	CCCC=C=O	ADIP2OOH	O=CCCCC(OO)C=O
PENTACID	CCCCC(O)=O	ADIP2CO	O=CCCCC(C=O)=O
HPMEPENT	OOCOC(CCCC)=O	ADIP2OH	O=CCCCC(O)C=O
C5SOZC	CCCCC1OOCO1	ADIP2O	O=CCCCC([O])C=O
BUCHOHOOH	OOC(O)CCCC	GLUTAL	O=CCCCC=O
HP1PEFORM	OOC(CCCC)OC=O	CO6HP5CO3	O=C(O[O])CCCC(OO)C=O
HP1PEPENT	OOC(CCCC)OC(CCCC)=O	CO65CO3H	O=C(OO)CCCC(C=O)=O
C5SOZC5	CCCCC1OOC(CCCC)O1	CO6HP5CO3H	O=C(OO)CCCC(OO)C=O
NC4H9O2	CCCCO[O]	CO6HP5CO2H	O=C(O)CCCC(OO)C=O
NC4H9OOH	CCCCOO	C6HOM1O2	O=C(OO)CCCC(O[O])C=O
NC4H9O	CCCC[O]	HCOC3CO3H	O=C(OO)CCCC=O
HO1C4O2	OCCCCO[O]	C6HOM1OH	O=C(OO)CCCC(O)C=O
HO1C4OOH	OCCCCOO	C6HOM1O	O=C(OO)CCCC([O])C=O
HOC3H6CHO	OCCCC=O	CO5HP4O2	O=CC(OO)CCCO[O]

43

HOC4H8OH	OCCCCO	HP5GLYOX	O=C(C=O)CCCOO
HO1C4O	OCCCC[O]	HP4CHO	O=CCCCOO
C4CHOAO2	CCCC(O[O])C=O	CO5HP4OOH	O=CC(OO)CCCOO
C4CHOAOOH	CCCC(OO)C=O	CO5HP4CHO	O=CCCC(C=O)OO
PGLYOX	CCCC(=O)C=O	CO5HP4OH	OCCCC(C=O)OO
C4CHO2O	CCCC([O])C=O	CO1HP5O2	O=CC(O[O])CCCOO
C6OH5O2	CCCCC(CO)O[O]	CO1HP5OH	OC(C=O)CCCOO
C6OH5OOH	CCCCC(CO)OO	CO1HP5O	[O]C(C=O)CCCOO
C4COMEOH	CCCCC(=O)CO		

Comments

[a] Organic species are listed. Simple inorganic species are represented as follows: Molecular hydrogen (H2), hydroxyl radical (OH), hydroperoxyl radical (HO2), hydrogen peroxide (H2O2), carbon monoxide (CO), ozone (O3) and atomic oxygen (O). Where required, the large excess concentrations of the reagents molecular oxygen, $[O_2]$, water, $[H_2O]$, water dimer, $[(H_2O)_2]$, and bath gas, $[M]$, appear as part of the rate coefficients in Table S4;

[b] Simplified Molecular Input Line Entry System (see: https://www.daylight.com/smiles/index.html);

[c] These are excited Criegee intermediates with varying amounts of excess internal energy, but their SMILES are indistinguishable from the corresponding stabilized Criegee intermediates.

References

Ammann, M., Cox, R. A., Crowley, J. N., Jenkin, M. E., Mellouki, A., Rossi, M. J., Troe, J., and Wallington, T. J.: Evaluated kinetic and photochemical data for atmospheric chemistry: Volume VI – heterogeneous reactions with liquid substrates, Atmos. Chem. Phys., 13, 8045-8228, 10.5194/acp-13-8045-2013, 2013.

Aschmann, S. M., Tuazon, E. C., Arey, J., and Atkinson, R.: Products of the Gas-Phase Reaction of O3 with Cyclohexene, J. Phys. Chem. A, 107, 2247-2255, 10.1021/jp022122e, 2003.

Bannan, T. J., Murray Booth, A., Le Breton, M., Bacak, A., Muller, J. B. A., Leather, K. E., Khan, M. A. H., Lee, J. D., Dunmore, R. E., Hopkins, J. R., Fleming, Z. E., Sheps, L., Taatjes, C. A., Shallcross, D. E. and Percival, C. J.: Seasonality of formic acid (HCOOH) in London during the ClearfLo campaign, J. Geophys. Res. Atmos., 122, 12,488-12,498 https://doi.org/10.1002/2017JD027064, 2017.

Bailey, P. S.: The reactions of ozone with organic compounds, Chem. Rev., 58, 925–1010, 1958.

Berasategui, M., Amedro, D., Vereecken, L., Lelieveld, J., and Crowley, J. N.: Reaction between CH3C(O)OOH (peracetic acid) and OH in the gas phase: a combined experimental and theoretical study of the kinetics and mechanism, Atmos. Chem. Phys., 20, 13541–13555, https://doi.org/10.5194/acp-20-13541-2020, 2020.

Calvert, J. G., Orlando, J. J., Stockwell, W. R., and Wallington, T. J.: The mechanisms of reactions influencing atmospheric ozone Oxford University Press, Oxford, UK, 2015.

Caravan, R.L., Vansco, M.F. and Lester, M.I.: Open questions on the reactivity of Criegee intermediates, Commun. Chem., 4, 44, https://doi.org/10.1038/s42004-021-00483-5, 2021.

Compernolle, S., Ceulemans, K., and Müller, J. F.: EVAPORATION: a new vapour pressure estimation method for organic molecules including non-additivity and intramolecular interactions, Atmos. Chem. Phys., 11, 9431-9450, 10.5194/acp-11-9431-2011, 2011.

Cox, R. A., Ammann, M., Crowley, J. N., Herrmann, H., Jenkin, M. E., McNeill, V. F., Mellouki, A., Troe, J., and Wallington, T. J.: Evaluated kinetic and photochemical data for atmospheric chemistry: Volume VII – Criegee intermediates, Atmos. Chem. Phys., 20, 13497-13519, 10.5194/acp-20-13497-2020, 2020.

Crowley, J. N., Ammann, M., Cox, R. A., Hynes, R. G., Jenkin, M. E., Mellouki, A., Rossi, M. J., Troe, J., and Wallington, T. J.: Evaluated kinetic and photochemical data for atmospheric chemistry: Volume V - Heterogeneous reactions on solid substrates, Atmos. Chem. Phys., 10, 9059-9223, 2010.

Dark, F. A., and Nash, T.: Comparative toxicity of various ozonized olefins to bacteria suspended in air, J. Hyg., 68, 245-252, 10.1017/S0022172400028710, 1970.

Deming, B. L., Pagonis, D., Liu, X., Day, D. A., Talukdar, R., Krechmer, J. E., de Gouw, J. A., Jimenez, J. L., and Ziemann, P. J.: Measurements of delays of gas-phase compounds in a wide variety of tubing materials due to gas–wall interactions, Atmos. Meas. Tech., 12, 3453-3461, 10.5194/amt-12-3453-2019, 2019.

Dollard, G. J. and Davies, T. J.: Observations of H_2O_2 and PAN in a rural atmosphere, Environ. Pollut., 75, 45-52, 1992.

Dollard, G. J., Dumitrean, P., Telling, S., Dixon, J. and Derwent, R. G.: Observed trends in ambient concentrations of C_2–C_8 hydrocarbons in the United Kingdom over the period from 1993 to 2004, Atmos. Environ., 41(12), 2559–2569, https://doi.org/10.1016/j.atmosenv.2006.11.020, 2007.

Donahue, N. M., Clarke, J. S., Demerjian, K. L., and Anderson, J. G.: Free-Radical Kinetics at High Pressure: A Mathematical Analysis of the Flow Reactor, The Journal of Physical Chemistry, 100, 5821-5838, 10.1021/jp9525503, 1996.

Druett, H. A., and May, K. R.: Unstable Germicidal Pollutant in Rural Air, Nature, 220, 395-396, 10.1038/220395a0, 1968.

Estimation Programs Interface Suite™ for Microsoft® Windows, v 4.11: https://www.epa.gov/tsca-screening-tools/epi-suitetm-estimation-program-interface, 2021.

Fleming, Z. L., Monks, P. S., Rickard, A. R., Bandy, B. J., Brough, N., Green, T. J., Reeves, C. E., and Penkett, S. A.: Seasonal dependence of peroxy radical concentrations at a Northern hemisphere marine boundary layer site during summer and winter: evidence for radical activity in winter, Atmos. Chem. Phys., 6, 5415–5433, https://doi.org/10.5194/acp-6-5415-2006, 2006.

Foreman, E. S., Kapnas, K. M. and Murray, C.: Reactions between Criegee intermediates and the inorganic acids HCl and HNO3: kinetics and atmospheric implications, Angew. Chem. Int. Ed., 55, 10419-10422, https://doi.org/10.1002/anie.201604662, 2016.

Hansel, A., Scholz, W., Mentler, B., Fischer, L., and Berndt, T.: Detection of RO2 radicals and other products from cyclohexene ozonolysis with NH4+ and acetate chemical ionization mass spectrometry, Atmos. Environ., 186, 248-255, https://doi.org/10.1016/j.atmosenv.2018.04.023, 2018.

Herndon, S. C., Villalta, P. W., Nelson, D. D., Jayne, J. T., and Zahniser, M. S.: Rate Constant Measurements for the Reaction of HO2 with O3 from 200 to 300 K Using a Turbulent Flow Reactor, J. Phys. Chem. A, 105, 1583-1591, 10.1021/jp002383t, 2001.

Hood, A. M.: Open-Air Factors in Enclosed Systems, J. Hyg., 72, 53-60, 1974.

Jenkin, M. E., Saunders, S. M., and Pilling, M. J.: The tropospheric degradation of volatile organic compounds: a protocol for mechanism development, Atmos. Environ., 31, 81-104, https://doi.org/10.1016/S1352-2310(96)00105-7, 1997.

Jenkin, M. E.: Trends in ozone concentration distributions in the UK since 1990: Local, regional and global influences, Atmos. Environ., 42, 5434–5445, https://doi.org/10.1016/j.atmosenv.2008.02.036, 2008.

Jenkin, M. E., Valorso, R., Aumont, B., Rickard, A. R., and Wallington, T. J.: Estimation of rate coefficients and branching ratios for gas-phase reactions of OH with aliphatic organic compounds for use in automated mechanism construction, Atmos. Chem. Phys., 18, 9297–9328, https://doi.org/10.5194/acp-18-9297-2018, 2018.

Jenkin, M. E., Valorso, R., Aumont, B., and Rickard, A. R.: Estimation of rate coefficients and branching ratios for reactions of organic peroxy radicals for use in automated mechanism construction, Atmos. Chem. Phys., 19, 7691-7717, 10.5194/acp-19-7691-2019, 2019.

Lakey, P. S. J., George, I. J., Whalley, L. K., Baeza-Romero, M. T., and Heard, D. E.: Measurements of the HO2 Uptake Coefficients onto Single Component Organic Aerosols, Environ. Sci. Technol., 49, 4878-4885, 10.1021/acs.est.5b00948, 2015.

Lakey, P. S. J., Berkemeier, T., Krapf, M., Dommen, J., Steimer, S. S., Whalley, L. K., Ingham, T., Baeza-Romero, M. T., Pöschl, U., Shiraiwa, M., Ammann, M., and Heard, D. E.: The effect of viscosity and diffusion on the HO2 uptake by sucrose and secondary organic aerosol particles, Atmos. Chem. Phys., 16, 13035-13047, 10.5194/acp-16-13035-2016, 2016.

Khan, M. A. H., Percival, C. J., Caravan, R. L., Taatjes, C. A., and Shallcross, D. E.: Criegee intermediates and their impacts on the troposphere, Environ. Sci.-Proc. Imp., 20, 437–453, 2018.

Le Breton, M., Bacak,, A., Muller, J. B. A., Xiao, P., Shallcross, B. M. A., Batt, R., Cooke, M. C., Shallcross, D. E., Bauguitte, S. J. -B. and Percival, C. J.: Simultaneous airborne nitric acid and formic acid measurements using a chemical ionization mass spectrometer around the UK: Analysis of primary and secondary production pathways, Atmos. Environ., 83, 166-175, https://doi.org/10.1016/j.atmosenv.2013.10.008, 2014.

Levin, V. A., Dolginow, D., Landahl, H. D., Yorke, C., and Csejtey, J.: Relationship of octanol/water partition coefficient and molecular weight to cellular permeability and partitioning in s49 lymphoma cells, Pharm. Res., 1, 259-266, 10.1023/A:1016393902123, 1984.

Lightfoot, P. D., Cox, R. A., Crowley, J. N., Destriau, M., Hayman, G. D., Jenkin, M. E., Moortgat, G. K., and Zabel, F.: Organic peroxy radicals: kinetics, spectroscopy and tropospheric chemistry, Atmos. Environ., 26A, 1805–1964, 1992.

Logan J. A., Prather M. J., Wofsy S. C. and McElroy M. B.: Tropospheric Chemistry: A global perspective. J. Geophys. Res., 86, 7210–7254, 1981.

McDonnell, G., and Russell, A. D.: Antiseptics and disinfectants: activity, action, and resistance, Clin. Microbiol. Rev., 12, 147-179, 1999.

McGillen, M. R., Carter, W. P. L., Mellouki, A., Orlando, J. J., Picquet-Varrault, B., and Wallington, T. J.: Database for the kinetics of the gas-phase atmospheric reactions of organic compounds, Earth Syst. Sci. Data, 12, 1203-1216, 10.5194/essd-12-1203-2020, 2020.

Mellouki, A., Ammann, M., Cox, R. A., Crowley, J. N., Herrmann, H., Jenkin, M. E., McNeill, V. F., Troe, J., and Wallington, T. J.: Evaluated kinetic and photochemical data for atmospheric chemistry: Volume VIII - gas phase reactions of organic species with four, or more, carbon atoms ($\geq$ C4), Atmos. Chem. Phys. Discuss., 2020, 1-22, 10.5194/acp-2020-940, 2020.

Mellouki, A., Ammann, M., Cox, R. A., Crowley, J. N., Herrmann, H., Jenkin, M. E., McNeill, V. F., Troe, J., and Wallington, T. J.: Evaluated kinetic and photochemical data for atmospheric chemistry: volume VIII – gas-phase reactions of organic species with four, or more, carbon atoms ($\geq$ C4), Atmos. Chem. Phys., 21, 4797-4808, 10.5194/acp-21-4797-2021, 2021.

Nash, T.: Physical aspects of air disinfection, Epidemiology and Infection, 49, 382-399, 10.1017/S0022172400066705, 1951.

Nguyen, T. B., Tyndall, G. S., Crounse, J. D., Teng, A. P., Bates, K. H., Schwantes, R. H., Coggon, M. M., Zhang, L., Feiner, P., Milller, D. O., Skog, K. M., Rivera-Rios, J. C., Dorris, M., Olson, K. F., Koss, A., Wild, R. J., Brown, S. S., Goldstein, A. H., de Gouw, J. A., Brune, W. H., Keutsch, F. N., Seinfeld, J, H., and Wennberg, P. O.: Atmospheric fates of Criegee intermediates in the ozonolysis of isoprene, Phys. Chem. Chem. Phys., 18, 10241–10254, 2016.

Osborn, D. L. and Taatjes, C. A.: The physical chemistry of Criegee intermediates in the gas phase, Int. Rev. Phys. Chem., 34, 309–360, 2015.

Passant, N. R.: Speciation of UK emissions of non-methane volatile organic compounds, AEA Technology Report ENV-0545, Culham, Abingdon, UK, 2002.

PORG: Ozone in the United Kingdom. Third Report of the UK Photochemical Oxidants Review Group, Department of the Environment, London. Published by Institute of Terrestrial Ecology, Bush Estate, Penicuik, Midlothian, EH26 0QB, UK. ISBN: 0 7058 1683 4, 1993.

PORG: Ozone in the United Kingdom. Fourth Report of the UK Photochemical Oxidants Review Group, Department of the Environment, Transport and the Regions, London. Institute of Terrestrial Ecology, Bush Estate, Penicuik, Midlothian, UK. ISBN: 0-870393-30-9, 1997. Executive summary available at: https://uk-air.defra.gov.uk/assets/documents/reports/empire/porg/fourth1.html.

Riva, M., Budisulistiorini, S. H., Zhang, Z., Gold, A., Thornton, J. A., Turpin, B. J., and Surratt, J. D.: Multiphase reactivity of gaseous hydroperoxide oligomers produced from isoprene ozonolysis in the presence of acidified aerosols, Atmos. Environ., 152, 314-322, https://doi.org/10.1016/j.atmosenv.2016.12.040, 2017.

Seeley, J. V., Jayne, J. T., and Molina, M. J.: High pressure fast-flow technique for gas phase kinetics studies, Int. J. Chem. Kin., 25, 571-594, https://doi.org/10.1002/kin.550250706, 1993.

Seeley, J. V., Jayne, J. T., and Molina, M. J.: Kinetic studies of chlorine atom reactions using the turbulent flow tube technique, J. Phys. Chem., 100, 4019-4025, 1996.

Sheps, L., Rotavera, B., Eskola, A. J., Osborn, D. L., Taatjes, C. A., Au, K., Shallcross, D. E., Khan, M. A. H. and Percival, C. J.: The reaction of Criegee intermediate CH$_2$OO with water dimer: primary products and atmospheric impact, Phys. Chem. Chem. Phys., 19, 21970–21979, 2017.

Tang, Y. S., Braban, C. F., Dragosits, U., Simmons, I., Leaver, D., van Dijk, N., Poskitt, J., Thacker, S., Patel, M., Carter, H., Pereira, M. G., Keenan, P. O., Lawlor, A., Conolly, C., Vincent, K., Heal, M. R., and Sutton, M. A.: Acid gases and aerosol measurements in the UK (1999–2015): regional distributions and trends, Atmos. Chem. Phys., 18, 16293–16324, https://doi.org/10.5194/acp-18-16293-2018, 2018.

Travagli, V., Zanardi, I., Valacchi, G., and Bocci, V.: Ozone and Ozonated Oils in Skin Diseases: A Review, Mediat. Inflamm., 2010, 610418, https://doi.org/10.1155/2010/610418, 2010.

Tuazon, E. C., Aschmann, S. M., Arey, J., and Atkinson, R.: Products of the Gas-Phase Reactions of O3 with a Series of Methyl-Substituted Ethenes, Environ. Sci. Technol., 31, 3004-3009, 10.1021/es970258y, 1997.

US-EPA: Estimation Programs Interface Suite™ for Microsoft® Windows, v 4.11. United States Environmental Protection Agency, Washington, DC, USA., 2012.

Vereecken, L., and Peeters, J.: Decomposition of substituted alkoxy radicals—part I: a generalized structure–activity relationship for reaction barrier heights, Phys. Chem. Chem. Phys., 11, 9062-9074, 10.1039/B909712K, 2009.

Vereecken, L., and Peeters, J.: A structure–activity relationship for the rate coefficient of H-migration in substituted alkoxy radicals, Phys. Chem. Chem. Phys., 12, 12608-12620, 10.1039/C0CP00387E, 2010.

Vereecken, L., Novelli, A., and Taraborrelli, D.: Unimolecular decay strongly limits the atmospheric impact of Criegee intermediates, Phys. Chem. Chem. Phys., 19, 31599-31612, 10.1039/C7CP05541B, 2017.

Vereecken, L., and Nozière, B.: H migration in peroxy radicals under atmospheric conditions, Atmos. Chem. Phys., 20, 7429-7458, 10.5194/acp-20-7429-2020, 2020.

Vereecken, L., Vu, G., Wahner, A., Kiendler-Scharr, A. and Nguyen, H. M. T.: A structure activity relationship for ring closure reactions in unsaturated alkylperoxy radicals, Phys. Chem. Chem. Phys., Advance Article, https://doi.org/10.1039/D1CP02758A, 2021.

Wang, Y., Chen, Z., Wu, Q., Liang, H., Huang, L., Li, H., Lu, K., Wu, Y., Dong, H., Zeng, L., and Zhang, Y.: Observation of atmospheric peroxides during Wangdu Campaign 2014 at a rural site in the North China Plain, Atmos. Chem. Phys., 16, 10985–11000, https://doi.org/10.5194/acp-16-10985-2016, 2016.

Watanabe, K., Kakuyama, S., Nishibe, M. and Michigami, S.: Measurements of atmospheric hydroperoxides at a rural site in central Japan, J. Atmos. Chem., 75, 71–84, https://doi.org/10.1007/s10874-017-9362-z, 2018.

Wu, Q. Q., Huang, L. B., Liang, H., Zhao, Y., Huang, D., and Chen, Z. M.: Heterogeneous reaction of peroxyacetic acid and hydrogen peroxide on ambient aerosol particles under dry and humid conditions: kinetics, mechanism and implications, Atmos. Chem. Phys., 15, 6851-6866, 10.5194/acp-15-6851-2015, 2015.

Zahardis, J., and Petrucci, G. A.: The oleic acid-ozone heterogeneous reaction system: products, kinetics, secondary chemistry, and atmospheric implications of a model system - a review, Atmos. Chem. Phys., 7, 1237-1274, 2007.

Zhang, X., He, S. Z., Chen, Z. M., Zhao, Y., and Hua, W.: Methyl hydroperoxide (CH_3OOH) in urban, suburban and rural atmosphere: ambient concentration, budget, and contribution to the atmospheric oxidizing capacity, Atmos. Chem. Phys., 12, 8951–8962, https://doi.org/10.5194/acp-12-8951-2012, 2012.